Bioenergetics (1973) **4**, 93–148

Molecular Basis for the Action of Macrocyclic Carriers on Passive Ionic Translocation Across Lipid Bilayer Membranes*

G. Eisenman, G. Szabo, S. G. A. McLaughlin and S. M. Ciani

Department of Physiology, UCLA School of Medicine, Los Angeles, California 90024

Introduction

Substantial energies in living cells are stored in ionic gradients across membranes. One of the central problems of biological energy transduction is that of understanding how these gradients arise and conversely, how the energy stored in such gradients is utilized to drive chemical reactions. These are two aspects of the reversible coupling of the energy of transmembrane ionic concentration gradients with the energy of chemical reactions—an electrochemical problem which may be thought of as involving, on the one hand, a mechanism for selective ion permeation and, on the other, a means of coupling that mechanism to the appropriate chemical reaction.

Relevant to such an understanding of the coupling between ion transport and chemical reactions should be the knowledge of the characteristics which are necessary and sufficient to produce a selective ion-translocating system, which is the principle subject of this paper. For example, schemes for metabolically-linked transport which involve conformational changes of the ion-transporter, as one step in the coupling process, from a state in which it is able to selectively bind and transport a particular ion or is rendered incapable of binding and transporting ions (cf. Skou, 1964; Whittam, 1967) require an understanding of the molecular mechanisms through which ion-selection and ion-transport arise. Similarly schemes which couple to chemical reactions the energy produced by the equilibration of an ionic (or redox) gradient (cf. Mitchell, 1961) must involve an understanding of the molecular structure of the membrane necessary to produce such selective ion equilibration. As an experimental fact, the ways in which monovalent cations exert their specific actions have been shown to follow the same

* Presented in part at the Symposium on Molecular Mechanisms of Antibiotic Action Protein Biosynthesis and Membranes, Granada, Spain, June, 1971. Supported by NSF Grant GB 16194 and USPHS Grants GM 17279 and NS 09931.

quantitative rules in metabolically dependent ionic accumulations, specific enzyme activating effects, and in purely passive membrane permeation (Eisenman, 1965).

The means by which specific ion translocation can be coupled to chemical reactions has been of considerable interest. Thus mechanisms for coupling the energy produced by electron and/or ionic transport to the production of ATP have been proposed and discussed by Lipmann (1946); Slater (1953); Lehninger (1965); Chance (1963); Boyer (1963, 1965); Lardy (1967); Green and Perdue (1966); Mitchell (1961, 1971); and others. In the direct chemical scheme the energy coupling occurs through the device of a chemical intermediate of high-energy nature generated by electron transport, which is used as a direct precursor for the formation of ATP. In electrochemical schemes, such as the "chemiosmotic hypothesis" of Mitchell (1971), coupling with the ionic gradient directly induces the formation of ATP. Detailed mechanisms by which the energy stored in ATP might be coupled to the production of ion gradients have been proposed and discussed by Patlak (1957), Skou (1964), Kepes (1964), Jardetsky (1966), Cockrell *et al.* (1967), Whittam (1967) and others. The reader interested in the reversible coupling between transport and chemical reactions is referred to Mitchell's excellent discussion (1971) as well as to other chapters in this volume. This chapter will deal with the simpler question of mechanisms by which ions can be selectively translocated across membranes under the passive conditions in which coupling to chemical reactions is not introduced. However, the ion-carrying molecules studied here can produce effects coupled to metabolism. For example, Cockrell *et al.* (1967) have shown that rotenone-treated mitochondria can synthesize ATP from ADP and inorganic phosphate when treated with valinomycin so as to enable utilization of the transmembrane K^+ gradient.

The membrane-active macrocyclic antibiotics to be considered here are particular members of a general class of amphiphilic molecules which are capable of interacting with cations through ligand oxygens, usually from the backbone of the molecule (Kilbourn *et al.*, 1967; Shemyakin *et al.*, 1969). Although typical molecules are cyclic, linear molecules can also be induced to fit around cations to form coordination complexes (Lardy *et al.*, 1967; Pressman, 1968). Complex formation comes about because the backbone oxygens of polypeptides, polyesters, or polyethers can interact with cations with energies comparable to those of hydration. Such molecules can therefore wrap around an ion and replace the hydration shell in such a way that a complex is formed in which the ion is sequestered in the polar interior of a molecule whose exterior is essentially lipophilic. The polar portion of the amphiphilic molecule decreases the electrostatic work of transferring the ion into the membrane interior; while the lipophilic portion

of the molecule interacts preferentially with the membrane. When the complex so formed has the appropriate dimension and conformation, it can behave as a mobile entity and thus act as a carrier of cations (Pressman *et al.*, 1967; Finkelstein and Cass, 1968; Eisenman, Ciani and Szabo, 1968). On the other hand, when the molecule has an appropriate conformation to form a stable trans-membrane structure with a polar interior, it can provide a way to pass ions through a channel across the membrane (Urry, 1971).

These two alternatives correspond to the carrier and neutral pore mechanisms IV and V of Eisenman's (1968) summary. An important distinction between the two types of action is that the former requires a liquid-like interior for the membrane, whereas the latter does not; and recent experiments by Krasne, Eisenman and Szabo (1971) indicate that these two mechanisms of operation can be distinguished by varying the fluidity of membranes. Furthermore, neutral molecules like gramicidin, which are thought to form pores in membranes, produced discrete jumps in membrane conductance; whereas molecules like monactin, which are thought to act as carriers, do not (Hladky and Haydon, 1970). The present paper will restrict its consideration to molecules thought to be carriers, particularly to those neutral molecules whose complexes bear the charge of the complexed-ion (in which case the charged complex is the principal carrier of electrical current). The principles underlying equilibrium selectivity should, however, also apply to "electrically silent" neutral complexes between cations and negatively charged antibiotics of the Nigericin-type.

For a considerable experimental range, the chemical reactions between carriers and carried ions not only occur sufficiently rapidly in the aqueous solutions, (cf. Eigen and Winkler, 1971), but also sufficiently rapidly at the membrane-solution interface, that these reactions can be considered to be at equilibrium relative to the rate of movement of the complexes across the membrane interior. In this situation, which may usefully be called the "equilibrium domain", an understanding of equilibrium chemistry suffices to account for the observable effects of these molecules on the membranes. Thus, in this domain, comparison of the theoretically expected and experimentally observed effects of valinomycin, four macrotetralide actins, and two cyclic polyethers on the electrical conductance and potential of phospholipid bilayer membranes (as well as on the equilibrium extraction of alkali picrates into organic solvents and the formation of ion-polyether complexes in aqueous solution) demonstrates that all salient effects of these molecules can be accounted for quantitatively from appropriate thermodynamic equilibrium constants.

There is, however, an experimental range in which equilibrium considerations alone do not account for the observed membrane properties of carriers. In this latter range, which has recently been

demonstrated by Läuger and Stark (1970) and Stark and Benz (1971) for strongly complexing carriers, strongly complexed ions and negatively charged lipids and by this laboratory for particular neutral lipids (Laprade *et al.*, 1972), the kinetics of the interfacial reactions become important, and thus in this range the system may be referred to as being in the "kinetic domain". A theoretical examination of the range of these domains will appear elsewhere (Ciani *et al.*, 1972), but Stark and Benz (1971) have demonstrated that both domains are observable for valinomycin, and we have also found this to be true for the macrotetralide actins (Laprade *et al.*, 1972). The present contribution confines its considerations, however, to experimental situations which fall within the equilibrium domain.

Five sets of new results are presented here and related to those from our previous studies of the macrotetralide actins.

The first section demonstrates that the effects of the depsipeptide, valinomycin, on phospholipid bilayer membranes are similar to those of the macrotetralide actins in the first order dependence of conductance on antibiotic (and cation) concentrations, and in the identity for pairs of cations (e.g. K vs. Na) of the numerical values of the permeability ratios, conductance ratios, and two-phase salt extraction equilibrium constant ratios. The range of applicability of our previous analysis for the macrotetralide actins (Ciani *et al.*, 1969, Eisenman *et al.*, 1969, Szabo *et al.*, 1969) is therefore extended to this depsipeptide.

The second section describes the considerably more complex effect on membranes of a cyclic polyether. For this molecule the conductance is found to depend on the 2nd and 3rd power of the polythere concentration. Also, the membrane conductance is only proportional to the concentration of permeant ion at low concentration (exhibiting a maximum and an inverse second order dependence at high concentrations), and the permeability ratios and conductance ratios are found to differ significantly at high concentrations of salt. Nevertheless, the present theory, when merely extended to allow for 2:1 and 3:1 polyether-cation complexes, successfully accounts for all of these observations. The range of applicability of our carrier treatment is therefore further extended to the cyclic polyethers.

The third section compares the quantitative cation selectivity patterns of valinomycin and the macrotetralides with each other and with that characteristic of biological membranes. Despite qualitative similarities in the sequences of ion effects, which are understandable in terms of the selectivity consideration of the last section, important quantitative differences are shown to exist among these molecules, and these differences may be used as "fingerprints" for certain characteristics of the molecule structure underlying cation permeation of the cell membrane. In particular, since the selectivity pattern of valinomycin for Li, Na, K, Rb, Cs and NH_4 is so close to that characteristic of cell

membranes, we speculate that the molecular environment around a cation in the cell membrane may involve six polypeptide carbonyl oxygens arrayed around the cation in a manner similar to the arrangement in valinomycin.

The fourth section examines certain general features of the equilibrium energetics underlying the equilibrium selectivity of neutral ion-sequestering molecules and demonstrates how, for isosteric complexes, the ratio of selectivities for membrane properties reflects the differences in hydration energies of the cation species vs. the differences in their interaction energies within the antibiotic molecules. It also shows how the same free energy differences underlie the selectivity between cations of the overall reaction (24) by which the present carriers solubilize cations in a membrane.

Finally, the fifth section extends a previous monopolar model for the selectivity of ion exchange sites (Eisenman, 1961, 1962, 1965) to the case of neutral, dipolar sites which are more appropriate as models for the carbonyl (or ether) oxygens which are the ligands in the present molecules.

Methods and Materials

The experimental apparatus and procedures used to characterize the electrical properties of bilayer membranes formed from mixtures of n-decane and various purified phospholipids have been described previously (Szabo *et al.*, 1969; McLaughlin *et al.*, 1970), as have the methods for characterizing salt extraction equilibria (Eisenman *et al.*, 1969). However, where necessary for clarity, additional details will be given. The cyclic polyethers were generously supplied by C. Pedersen and H. K. Frensdorff of E. I. duPont de Nemours Co. The macrotetralide actins were gifts from Dr. H. Bickel of CIBA and Miss B. Stearns of Squibb. Valinomycin was a gift from Dr. G. Mallett of the Eli Lilly Co., and also was purchased from Calbiochem (the former sample had 90% the activity of the latter, presumably due to prolonged storage). Phosphatidyl ethanolamine and phosphatidyl glycerophosphate were gifts from J. Law and M. Kates.

The Effects of Valinomycin on the Electrical Properties of Bilayer Membranes and on Two-Phase Salt Extraction Equilibria

The purpose of this section is to extend and make more quantitative the previous characterizations of the effects of valinomycin on bilayer membrane potential and conductance (Mueller and Rudin, 1967; Lev and Buzhinsky, 1967; Andreoli *et al.*, 1967), as well as on two-phase salt extractions (Pressman, 1968), in order to test whether or not the theoretical considerations we have previously applied for the macrotetralide actins also hold for valinomycin. We shall show that, as with

the macrotetralides, the principal effects of valinomycin on membranes are completely understandable in terms of the ability of this molecule to form a 1:1 complex with cations. Moreover, we shall verify that the ability of valinomycin to mediate the membrane permeability and conductance of the alkali metal cations is accurately accounted for by the appropriate equilibrium thermodynamic parameters (Eisenman *et al.*, 1969), as measured in two-phase salt extraction experiments. It will be helpful, before presenting experimental data to summarize briefly the salient theoretical expectations of our previously developed carrier treatment (Eisenman *et al.*, 1968; Ciani *et al.*, 1969) in order to provide a basis for interpreting the data for valinomycin and also to provide background for the subsequent extension to the cyclic polyethers in the second section.

Theoretical Considerations

For the purpose of this paper it will suffice to consider only the expectations for neutral lipids, uncomplicated by effects of charged polar head groups (Lesslauer *et al.*, 1967; McLaughlin *et al.*, 1970; Neumcke, 1970; Szabo *et al.*, 1972a), which are treated in detail elsewhere (McLaughlin *et al.*, 1970). For a membrane of the dimensions of a phospholipid bilayer (i.e., one whose thickness is less than the apparent Debye length within the hydrocarbon phase), we have deduced (Ciani *et al.*, 1969) that the cation-antibiotic complexes, IS^+, should be the major charge-carrying species within the membrane, where they are present as an excess space charge. (The concentration of these species within the membrane is sufficiently high that it determines the membrane's electrical properties, but low enough i.e. $C_{is}^* < 5 \times 10^{-5}$ M (Neumcke and Läuger, 1970) for the constant-field approximation to hold).

By integrating the Nernst-Planck flux equations for these complexes the simple equation

$$V_0 = \frac{RT}{F} \ln \frac{a_i' + \beta a_j'}{a_i'' + \beta a_j''}, \tag{1}$$

for the membrane potential, V_0, at zero current was deduced. Equation (1) expresses the potential difference between the aqueous solutions in terms of the activities, a_i', a_j', a_i'', a_j'', of the ions, I^+ and J^+, in the aqueous solutions on the two sides (′) and (″) of the membrane and a constant β, which is formally equivalent to the permeability ratio, P_j/P_i, of the Goldman-Hodgkin-Katz equation (Goldman, 1943; Hodgkin and Katz, 1949), being defined as

$$\beta = \frac{P_j}{P_i} = \frac{u_{js}^* k_{js} K_{js}^+}{u_{is}^* k_{is} K_{is}^+}, \tag{2}$$

where u_{js}^*/u_{is}^* is the ratio of the mobilities of the JS^+ and IS^+ complexes in the membrane, k_{js}/k_{is} is the ratio of the partition coefficients of the

complexes and K_{js}^{+}/K_{is}^{+} is the ratio of the equilibrium constants for the formation of the complexes in aqueous solution.* No assumptions as to electroneutrality or as to profiles of potential or concentration were necessary to obtain this result, but we did assume that the equilibria at the membrane-solution interfaces were not perturbed by the flux of the complexes. Equation (1) is expected to hold for all the experimental conditions of this section.†

The membrane conductance, measured on the limit of vanishingly small applied voltage, was also deduced by evaluating the concentration profiles through integration of the Poisson–Boltzmann equation for the equilibrium situation where the aqueous solutions on both sides of the membrane have the same composition (Ciani *et al.*, 1969).‡ For the case of a single cation, J^{+}, the membrane conductance in the limit of zero current, $G_0(J)$, is given by:

$$G_0(J) = \left[\frac{F^2}{d} u_{js}^{*} k_{js} K_{js}^{+}\right] C_s^{Tot} a_j \frac{1}{1+K_{js}^{+} a_j}, \tag{3}$$

which, in the (usually encountered) limit of sufficiently low salt concentration that $K_{js}^{+} a_j \ll 1$, reduces to the simpler form

$$G_0(J) = \left[\frac{F^2}{d} u_{js}^{*} k_{js} K_{js}^{+}\right] C_s^{Tot} a_j. \tag{4}$$

Equations (3) and (4) indicate that the membrane conductance is expected to be proportional to the total aqueous concentration of antibiotic, C_s^{Tot}, and also to be proportional to the activity of the cation in the solution, a_j, at least at low salt concentrations. Taking the ratios of membrane conductances for J^{+} vs. I^{+} from equation 4,

$$\frac{G_0(J)}{G_0(I)} = \frac{u_{js}^{*} k_{js} K_{js}^{+}}{u_{is}^{*} k_{is} K_{is}^{+}}, \tag{5}$$

and comparing with the permeability ratios of equation (2), it is immediately apparent that the conductance ratios should equal the permeability ratios:

$$\frac{G_0(J)}{G_0(I)} = \frac{P_j}{P_i} \tag{6}$$

* The parameters K_{js}^{+}, k_{js} and K_j are defined in equations (24) to (28).

† Space does not permit a more extensive discussion of the range of applicability of equation (1) here other than to remark that in an analysis published elsewhere, Szabo, Eisenman and Ciani (1970) verified for the macrotetralides that equation (1) holds generally regardless of differences in antibiotic concentration in the solutions on the two sides of the membrane and the degree of complexation in the aqueous solutions, provided only that the rate of diffusion of the neutral, uncomplexed antibiotic within the membrane is rapid compared to its diffusion through the unstirred aqueous layers adjacent to the membrane and or the membrane-solution interface, as is expected for valinomycin as well as for the macrotetralides.

‡ We have assumed the diffusion of IS^{+} in the membrane to be the rate-limiting step for ion transport. (This is not to be confused with the rapid diffusion mentioned in the previous footnote for the neutral, uncomplexed species, S). It should be noted that the application of the present equilibrium considerations to steady-state measurements is valid only under this condition (Läuger and Stark, 1970; Markin *et al.*, 1969a,b; and Ciani *et al.*, 1972).

This expectation was extensively tested and verified for the four macrotetralides (Szabo *et al.*, 1969); it will be verified here for valinomycin as well.

We also showed (Eisenman, Ciani and Szabo, 1969) that the equilibrium constants, K_i, for the extraction of a salt composed of monovalent ions I^+ and X^- from the aqueous phase into a bulk solvent phase by the antibiotic molecule, S, is expressable in terms of the previous parameters as

$$K_i = \frac{k_{is} K_{is}^+ k_x}{k_s} \tag{7}$$

where k_x and k_s are the partition coefficients of the anion and antibiotic, respectively.*

Taking the ratio of these salt extraction constants for J^+ and I^+, K_j/K_i, it is seen that

$$\frac{K_j}{K_i} = \frac{k_{js} K_{js}^+}{k_{is} K_{is}^+}, \tag{8}$$

since both k_x and k_s cancel for a given solvent in the case of a given anion and antibiotic. Comparing equation (8) with equations (2) and (5) for the permeability ratios and conductance ratios of a membrane (made of the same solvent), we see that

$$\frac{P_j}{P_i} = \frac{G_0(\mathrm{J})}{G_0(\mathrm{I})} = \frac{u_{js}^* k_{js} K_{js}^+}{u_{is}^* k_{is} K_{is}^+}, \tag{9}$$

or

$$\frac{P_j}{P_i} = \frac{G_0(\mathrm{J})}{G_0(\mathrm{I})} = \frac{u_{js}^* K_j}{u_{is}^* K_i}. \tag{10}$$

Equation (10) explicitly relates the ratio of equilibrium constants, K_j/K_i, for salt extraction into a given solvent to the electrical properties of a thin membrane made of the same solvent; while equation (9) relates the permeability and conductance ratios to the ratio of aqueous formation constants for the complex, K_{js}^+/K_{is}^+, times the ratio of partition coefficients of the complex between water and the membrane, k_{js}/k_{is}, and the ratio of the mobilities of these complexes in the membrane, u_{js}^*/u_{is}^*. Note that such characteristics as the size and shape of the complex could vary from cation to cation, and the above conclusions would still hold since no particularizing assumptions have been made as yet concerning the physical properties of the complexes. The comparison between membrane and bulk phases made in equation (10) would, however, necessitate that the membrane be made of the same solvent as the bulk phase.

* I.e., for the reactions: $I^+ + X^- + S^* \overset{K_I}{\rightleftharpoons} IS^{+*} + X^{-*}$ defined in Equation (25).

To circumvent this difficulty, we introduced the postulate of "isostericity", in which we assumed that the overall size and shape of the complex, as well as its externally-viewed electron distributions, was the same for all cations. In this case, the interaction energy with the solvent of the complex should not vary with the particular cation species bound; and the partition coefficients of all complexes are expected to be the same for any solvent so that by

$$\frac{k_{js}}{k_{is}} \cong 1, \tag{11}$$

for all solvent (and phospholipid bilayer) compositions.

This result immediately allows us to deduce, on inserting equation 11 in equation 8, that

$$\frac{K_j}{K_i} \cong \frac{K_{js}^+}{K_{is}^+}. \tag{12}$$

Thus, the ratios of salt extraction equilibrium constants, K_j/K_i should be not only independent* of the solvent in which they are measured but, moreover, may be taken as a measure of the ratio of K_{js}^+/K_{is}^+, the ratio of stability constants for complex formation in aqueous solution.

Similarly, the mobility ratios of isosteric complexes should be independent of the composition of the membrane, being given by

$$\frac{u_{js}^*}{u_{is}^*} \cong 1, \tag{13}$$

regardless of the particular cation species bound, since all isosteric complexes are also expected to be indistinguishable with regard to their mobilities. Inserting equation (13) in equation (10), and recalling equation (12), the remarkably simple set of relationships was found

$$\frac{P_j}{P_i} = \frac{G_0(\mathrm{J})}{G_0(\mathrm{I})} = \frac{K_j}{K_i} = \frac{K_{js}^+}{K_{is}^+}, \tag{14}$$

Equation (14) contains the principal theoretical expectations which we have previously verified for the macrotetralides and which we will now test for valinomycin. In particular, equation (14) predicts: first, that membrane conductance ratios and permeability ratios should be identical for a given pair of cations (e.g. Na^+ vs. K^+); second, that the equilibrium constant ratios measured by salt extraction should also be identical to the permeability and conductance ratios, regardless of the composition of membrane or solvent; and third, that these ratios

* This independence has been verified in model solvents for the membrane interior varying in dielectric constant from 2 (hexane) to 9 (dichloromethane). An analysis of the free energies underlying equation (12) will be presented in a further section. To avoid confusion with stability constants measured in other solvents the reader should recall that the reference state for the cations both for the 2-phase salt extraction equilibrium constant, K_j, and for the aqueous stability constant, K_{js}^+, is always the cation in water at infinite dilution.

should reflect the ratios of stability constants of the complexes in aqueous media.* From Equation (14) it is apparent why for isosteric complexes the choice of model solvent for the salt extraction studies is not critical.

The Experimentally Observed Effects of Valinomycin

There is a general agreement that the effect of valinomycin on bilayer membranes is characterized by a first power dependence of membrane conductance on antibiotic concentration (Tosteson *et al.*, 1968, McLaughlin *et al.*, 1970, Stark and Benz, 1971). This is in accord with the expectation of equations (3) and (4) and is illustrated in Fig. 1 by the slope of 1 for the logarithm of membrane conductance as a function of the logarithm of valinomycin concentration for three

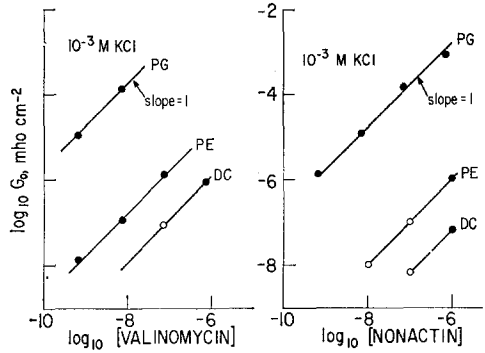

Figure 1. The first power dependence of membrane conductance on Valinomycin concentration (left) and Nonactin concentration (right). The experimentally observed conductances are indicated by data points; and the lines are drawn with a slope of 1. Open circles indicate values extrapolated from measurements made at higher KCl concentrations.

different lipids (the neutral lipid 7-dehydrocholesterol (DC), the amphoteric lipid phosphatidyl ethanolamine (PE), and the negatively charged lipid phosphatidyl glycerol (PG)). For comparison, the closely similar behavior of the typical macrotetralide, nonactin, is illustrated in the right hand portion of Fig. 1. (Note the close correspondence for valinomycin and nonactin of the dependence of effectiveness on lipid composition, as indicated by the identical displacements from lipid to lipid of the conductances due to these two antibiotics.)

The proportionality between membrane conductance and concentration of permeant cation, expected from equation (4) for uncharged

* Of course, this does not imply that any substantial number of complexes are actually present in the aqueous phase in the experimental concentration range. Indeed, to the extent that equation (4), rather than equation (3) is observed to describe the membrane conductance satisfactorily, we may deduce that a negligible fraction of antibiotic is complexed to cations in the usual aqueous media. Nevertheless, the free energies underlying the selectivity determined by the K_{Js}^{+}/K_{ts}^{+} ratios are the same as those underlying the selectivity determined by the K_J/K_t, P_J/P_i and $G^0(\mathrm{J})/G^0(\mathrm{J})$ ratios, discussed later.

lipids, is also verified in Fig. 2 for DC and PE by the fairly wide range of conditions over which simple proportionality holds, as judged by the lines of slope 1. Such a strict proportionality when ionic strength is allowed to vary (as in Fig. 2) is expected only for neutral lipids. For charged lipids, deviations from simple proportionality are expected (and observed) with varying ionic strength in accord with the expectations of diffuse double layer theory (cf. Lesslauer *et al.*, 1967 and McLaughlin *et al.*, 1970). These can lead to an apparent 0th power dependence for a negatively charged lipid or an apparent 2nd power

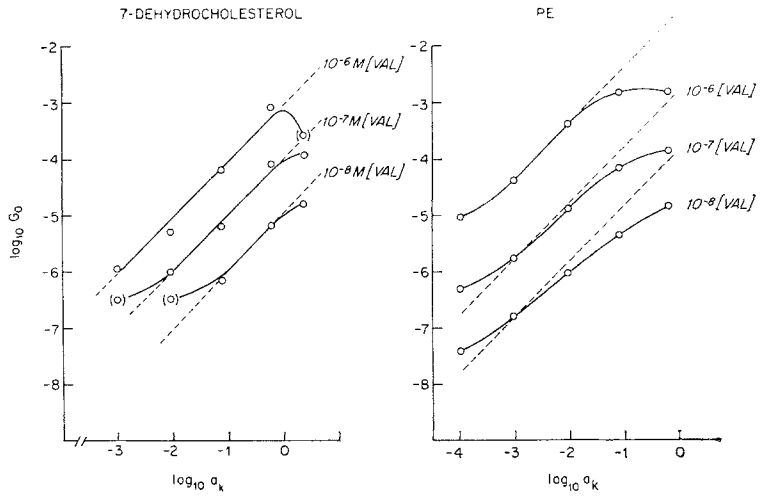

Figure 2. The proportionality between Valinomycin-mediated membrane conductance and concentration of permeant cation K^+ for the uncharged lipids 7 Dehydrocholesterol (DC) and Phosphatidyl ethanolamine (PE). Experimentally observed conductances are indicated by data points, while the lines are drawn with a slope of 1.

dependence for a positively charged lipid (Szabo *et al.*, 1970, p. 127 ff., and particularly equation (5) of McLaughlin *et al.*, 1970). This probably accounts for the departures from simple proportionality reported for valinomycin (Tosteson, 1968, Lieberman and Topaly, 1968, and Lieberman, Pronevich and Topaly, 1970). These effects can be overcome by holding ionic strength constant (Szabo *et al.*, 1969, Fig. 11). Indeed, Stark and Benz (1971) have demonstrated, in very carefully executed experiments at constant ionic strength, the strict proportionality between membrane conductance and K^+ concentration for the negatively charged lipid, phosphatidyl inositol, as well as for the neutral lipid, phosphatidyl choline.

All of the above observations are consistent with the postulate that valinomycin acts as a carrier of cations across bilayer membranes by forming 1:1 lipid soluble complexes with alkali metal cations, as do the macrotetralide actins. This similarity between valinomycin and

the macrotetralide actins has recently been verified in experiments designed to test the carrier hypothesis by reversibly freezing and melting bilayer membranes (Krasne *et al.*, 1971). In these experiments it was found that the membrane effects of both valinomycin and nonactin were obliterated at the same temperature by solidifying the membranes. By contrast, the membrane effects of gramicidin A, a postulated channel former (Hladky and Haydon, 1970; Goodall, 1970), were unaltered by solidifying the membrane.*

Selectivity Among Alkali Metal Cations

The relative ability of valinomycin to mediate the effects of the alkali metal cations on membranes were first described by Mueller and Rudin (1967), who found the sequence $Rb > K > Cs > Na > Li$ both for membrane potential and for membrane conductance. A characterization of the effects of these ions on membrane potential, in agreement with that of Mueller and Rudin but in considerably greater detail, was presented by Lev and Buzhinsky (1967). This sequence was also confirmed by Andreoli *et al.* (1967). The same sequence of cation potencies was found by Pressman (1968) for the effectiveness of valinomycin in extracting the thiocyanate salts of the alkali metals into toluene-butanol. Thus, it is seen that, at least qualitatively, the similar sequence of cation effects on permeability ratios, conductance ratios, and salt extraction potencies indicates that the expectations of Equation (14) are being fulfilled for valinomycin. To test this quantitatively we have carried out salt extraction experiments with valinomycin in exactly the same manner as previously used for the macrotetralides (Eisenman *et al.*, 1969).

Figure 3 presents the results of two sets of measurements for valinomycin for the extraction of the picrate salts of the alkali metal cations into the solvent dichloromethane.† The equilibrium constants, K_i, characteristic of these measurements are presented in the first two columns of Table I; and the last column gives the average ratios, K_i/K_K, of salt extraction equilibrium constants relative to K^+. The sequence $Rb > K > Cs > Na > Li$ is confirmed, and the close quantitative agreement of the ratios of our salt extraction equilibrium

* Not only is valinomycin similar to the macrotetralide actins in its above mentioned effects, but also in the shape of its current-voltage characteristic, which we find to have a hyperbolic sine characteristic closely similar to that previously described for monactin by Szabo *et al.* (1969, Fig. 1), except at high salt concentrations. Such an increasing conductance with increasing voltage was first noted for valinomycin by Lev in 1966 (personal communication) and is also apparent in the published data of Andreoli *et al.* (1967, Fig. 3). By contrast, a current-limiting I–V curve has been reported as typical by Lieberman and Topoly (1968); and, indeed, we have seen this at very high KCl concentrations. Since the shape of the I–V relationship for valinodimycin also depends on lipid composition(Stark andBenz, 1971), the apparent contradictions in the literature are understandable.

† This solvent has previously been established (Eisenman *et al.*, 1969) for the macrotetralides, to be satisfactory for measuring the desired equilibrium constant K_i of equation (7), without complication from ion pairing with the picrate anion.

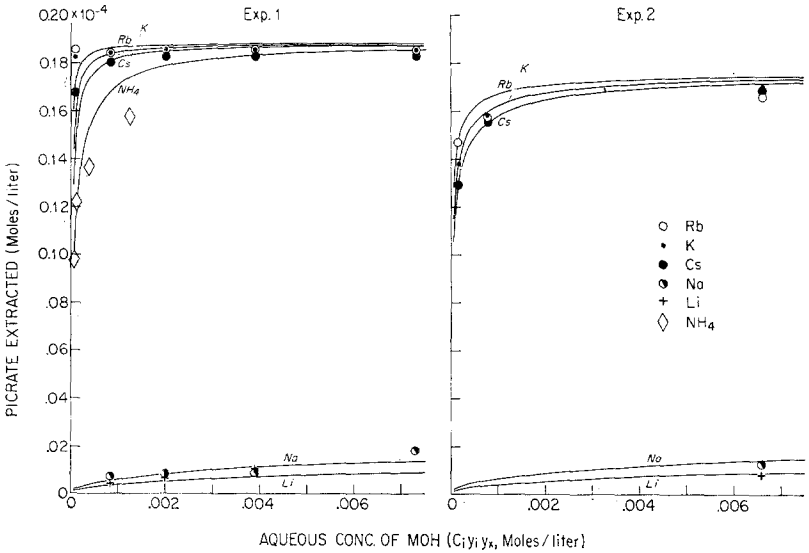

Figure 3. Extraction of alkali picrates into dichloromethane by valinomycin. The concentration of picrate extracted into the organic phase at equilibrium is plotted as a function of the aqueous concentration of MOH (corrected for activity coefficient effects). The units of the ordinate and abscissa are moles per liter. The points are experimentally observed, the curves theoretically calculated (according to Eisenman *et al.*, 1969, equation (28)) with the values of the equilibrium constants K_i given in the first two columns of Table I. The left-hand figure corresponds to experiment (1) and the right-hand figure corresponds to experiment (2) carried out under the following experimental conditions: Expt. (1), initial picrate concentrations = 10^{-4} M, initial valinomycin concentration $0{\cdot}188 \times 10^{-4}$ M, aqueous phase 10 ml, organic phase 10 ml; Expt. (2), initial picrate concentration = 10^{-4} M, initial valinomycin concentration $0{\cdot}176 \times 10^{-4}$ M, aqueous phase 2 ml, organic phase 10 ml. For methods of calculation see Eisenman *et al.*, 1969.

TABLE I. Equilibrium constants for valinomycin's ability to extract picrates into dichloromethane

	K_i	K_i	K_i/K_K
	Expt. (1)	Expt. (2)	Average
Rb	22,000	19,000	1·95
K	10,800	10,000	1·0
Cs	6,300	6,600	0·62
NH_4	2,00	—	0·19
Na	0·15	0·2	0·000017
Li	0·06	0·07	0·000007

The experimental conditions were the same as in Tables 4 and 14 of Eisenman *et al.*, 1969, using valinomycin from E. Lilly. The initial conditions for the two experiments were:

Expt. (1): $C^{\text{In}}_{\text{Picrate}} = 10^{-4}$ M, $C^{\text{In}}_{\text{Val}} = 0{\cdot}2 \times 10^{-4}$ M, $V = 10$ ml
$V^* = 10$ ml.

Expt. (2): $C^{\text{In}}_{\text{Picrate}} = 10^{-4}$ M, $C^{\text{In}}_{\text{Val}} = 0{\cdot}176 \times 10^{-4}$ M, $V = 2$ ml
$V^* = 10$ ml.

constants with literature values for the permeability ratios and conductance ratios for bilayers can be seen in Table II. Note the numerical correspondence between our K_i/K_K ratios in column (1) and the corresponding permeability and conductance ratios from the publications of Lev and Buzhinsky in column (2) and of Mueller and Rudin in columns (3) and (4). This agreement verifies that the important equality, equation (14), holds for valinomycin.*

TABLE II. Test of the identity between permeability ratios, conductance ratios, and salt extraction equilibrium constant ratios for valinomycin

	K_i/K_K*	P_i/P_K†	P_i/P_K‡	$G^0(K)/G^0(K)$†
Li	0·000007	(<0·012)	(0·0025)	(<0·005)
Na	0·000017	(<0·014)	(0·0035)	(<0·006)
K	1·0	1·0	1·0	1·0
Rb	1·95	1·9	2·3	1·5
Cs	0·62	0·44	0·53	0·25
NH_4	0·19	—	—	—

Note that the parenthesized quantities were obtained at neutral pH under conditions in which the H^+ ion can make a substantial contribution to the potential and conductance whereas the salt extraction equilibrium constants were obtained at alkaline pH, where the effects of H^+ are minimized. For this reason the data for the membranes may overestimate the relative permeabilities of the ions Li and Na, and the values listed must be considered to be maximum values for the permeabilities of these ions.

* From Table I.

† From Data of Lev and Buzhinsky, 1967, at 23°C and at 0·1 M salt (except H^+ at 0·001 M).

‡ From the data of Mueller and Rudin, 1967, at room temperature and 0·05 M salt for P_i/P_K (conductance ratios obtained at 35°C).

From all the above findings, it seems reasonable to postulate that valinomycin and the macrotetralide actins behave in the same general way and may be usefully regarded as members of the same class of carriers; they both form 1:1 complexes with cations and differ only quantitatively in the numerical values of the constants underlying their selectivity among cations, as will now be considered more extensively.

A Further Comparison of the Effects of Valinomycin with Those of the Macrotetralide Actins

With these results in hand, it is possible to compare in some detail the parameters underlying the effects of valinomycin with the corresponding parameters for the macrotetralide actins. Table III sum-

* Incidentally, the potential selectivity constants measured by Simon and his colleagues (1970) for valinomycin in thick electrodes made of diphenyl ether are also in close agreement with the data of Table II, as can be seen by comparison with his potential selectivity constants, referred to K^+, of: Li (<0.00021), Na (<0.00026), K (1), Rb (1·9), Cs (0·48), NH_4 (0·012), H (0·000056).

TABLE III. Salt extraction equilibrium constants, K_i, for the macrotetralide actins and comparison of the extraction ratios K_i/K_K with the conductance and permeability ratios for bilayer membranes

		K_i*	K_i/K_K*	P_i/P_K†	$G^0(I)/G^0(K)$†
Nonactin	Li	0·05	0·00026	<0·001	0·00042
	Na	3·2	0·017	0·0071	0·0067
	K	190	1	1	1
	Rb	90	0·47	0·58	0·58
	Cs	11·5	0·061	0·033	0·039
	NH_4	9,000	47	8‡	5‡
Monactin	Li	0·10	0·00012	<0·0005	0·00025
	Na	8	0·0096	0·0075	0·0048
	K	850	1	1	1
	Rb	290	0·34	0·5	0·34
	Cs	25	0·029	0·024	0·014
	NH_4	16,000	19	—	—
Dinactin	Li	0·15	0·000076	<0·00058	0·0002
	Na	25	0·012	0·0067	0·0081
	K	2,000	1	1	1
	Rb	800	0·40	0·42	0·48
	Cs	46	0·023	0·014	0·012
	NH_4	24,000	12	—	—
Trinactin	Li	0·23	0·000059	<0·00058	0·000033
	Na	42	0·011	0·009	0·0042
	K	4,000	1	1	1
	Rb	1,170	0·29	0·32	0·38
	Cs	75	0·019	0·015	0·013
	NH_4	46,000	11	4‡	3·5‡

* Eisenman *et al.*, 1969, Table 15.
† Szabo *et al.*, 1969, Table 5.
‡ Data of Laprade, Szabo and Eisenman for phosphatidyl ethanolamine.

marizes data for the macrotetralides from our previous studies and also includes data for NH_4^+ from work in progress in our laboratory by Raynald Laprade. The first column presents the salt extraction equilibrium constants, characterized for dichloromethane under the same experimental conditions as for valinomycin in Table II. These K_i values may therefore be directly compared to those for valinomycin. The second, third and fourth columns compare the values of the ratios K_i/K_K, P_i/P_K, and $G^0(I)/G^0(K)$, respectively. Notice the excellent agreement in the numerical values for all three of these ratios in agreement with equation (14).*

Comparison of the values of K_i for the macrotetralides in Table III with those for valinomycin in Table I indicate that valinomycin is

* Incidentally, these ratios agree closely with the potential selectivity constants measured by Simon and his colleagues (1971) for thick electrodes made from nonactin in Nujol/2-octanol, for which, the selectivities relative to K^+, were: Li (0·00056), Na (0·0067), K (1·0), Rb (0·42), Cs (0·031), NH_4 (2·5), H (0·018).

considerably more effective in its ability to extract the salts of the larger alkali metal cations than even the most effective macrotetralide, trinactin. This is illustrated in Fig. 4 where the values of log K_i are plotted for the antibiotics ranked in sequence: Nonactin, Monactin, Dinactin, Trinactin, Valinomycin.

The relative abilities of valinomycin and the macrotetralides to extract K^+ into a model solvent correlate surprisingly well with the relative effect of these molecules in the membrane's K^+ conductance. From the salt extraction data of Tables I and III, the ratio, K_j^V/K_j^M, is about 12. This correlates quite closely with the finding by Stark and Benz (1971) that the K^+ conductance produced by valinomycin is about 10 times as high as that produced by monactin under identical experimental conditions (a bilayer membrane made from dioleyl lecithin in the presence of 10^{-7} M antibiotic and 1·0 M ionic strength). This rather close correspondence may be somewhat fortuitous, as can be seen by comparison of the explicit expectations for the relationship between membrane conductance for a given antibiotic and its salt extraction equilibrium constant, which can be obtained from equation (4), on insertion of equation (7), to yield:

$$G_0(J) = \left[\frac{F^2}{d}\frac{C_s^{Tot} a_j}{k_x}\right] u_{js}^* k_s K_j. \tag{15}$$

The bracketed quantity in equation (15) will cancel when comparing ratios of membrane conductances with ratios of salt extractions carried out for two different antibiotics under the same experimental conditions. Therefore, if the ratio of conductances for valinomycin (denoted by the superscript V) and monactin (denoted by the superscript M), are compared, one obtains the expectation

$$\frac{G_0^V(J)}{G_0^M(J)} = \frac{u_{js}^{*V} k_s^V K_j^V}{u_{js}^{*M} k_s^M K_j^M}. \tag{16}$$

Since $G_0^V(J)/G_0^M(J) = 10$, and $K_j^V/K_j^M = 12$, equation (16) implies that $u_{js}^{*V} k_s^V / u_{js}^{*M} k_s^M = 1/1{\cdot}2$. However, Stark and Benz also estimated the partition coefficients for dioleyl lecithin to be 6000 for monactin and 25,000 for valinomycin for this lipid, indicating that $k_s^V/k_s^M = 4{\cdot}2$. Taken literally this would imply that the mobility of the valinomycin complex is considerably less than that of the monactin complex if equation (16) is valid.*

It is also of some interest to try to deduce the relative values of K_{is}^+ for valinomycin vs. monactin from the relative values of K_i. This would be particularly pertinent to assessing whether effects due to complex

* However, it would not be unprecedented for the high partition coefficient for valinomycin to reflect additional interactions (possibly even a surface adsorption (Colacicco, 1969)) which might diminish its mobility. (Such opposing effects are characteristic of the movement of cations in glass, where the most strongly preferred cation is the least mobile (Eisenman, 1967).)

formation in the aqueous solution might be expected to occur at lower salt concentrations with valinomycin than with the macrotetralides. A difference in aqueous stability constants has implications for the effects of these molecules on bilayer membranes, as should be apparent from equation (3) in which it can be seen that when the term $K_{is}^{+}a_i$ is not negligible compared to unity, deviations are expected from the linear dependence of membrane conductance on salt concentration. Such an effect is a direct consequence of the fact that, when ion-carrier association in the aqueous phases becomes appreciable (i.e. $K_{is}^{+}a_i \geqslant 1$), not all of the carrier molecules are present in the free, uncomplexed form. Since the membrane conductance is proportional to the concentration of the free carrier as well as that of the salt, aqueous association results in a deviation from the proportionality seen otherwise between membrane conductance and salt concentration.

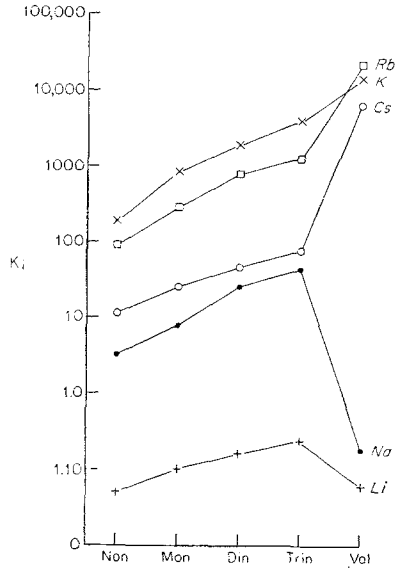

Figure 4. Summary of salt extraction equilibrium constants for the macrotetralides and valinomycin. The ordinate plots the logarithm of the values of K_i for the indicated cations as a function of the series of antibiotic molecules indicated on the abscissa.

The ratio of aqueous complex formation constants for valinomycin vs. the macrotetralides (denoted by M) can be deduced from equation (7) as:

$$\frac{K_{is}^{+\mathrm{V}}}{K_{is}^{+\mathrm{M}}} = \frac{K_i^{\mathrm{V}}}{K_i^{\mathrm{M}}} \frac{k_s^{\mathrm{V}}}{k_s^{\mathrm{M}}} \frac{k_{is}^{\mathrm{M}}}{k_{is}^{\mathrm{V}}}. \tag{17}$$

It seems plausible to assume that $k_s^{\mathrm{V}} k_{is}^{\mathrm{M}} / k_s^{\mathrm{M}} k_{is}^{\mathrm{V}} = 1$, in which case, equation (17) becomes:

$$\frac{K_{is}^{+\mathrm{V}}}{K_{is}^{+\mathrm{M}}} \simeq \frac{K_i^{\mathrm{V}}}{K_i^{\mathrm{M}}}, \tag{18}$$

indicating that the ratio of aqueous complex formation constants should be equal to the ratios of the salt extraction equilibrium constants. To the extent that this is true, Figure 4 can then serve to predict the relative values of K_{is}^{+}.

The Cyclic Polyethers, Bis Cyclohexyl-18-*Crown*-6 (*XXXI*) *and Bis*(*T-Butyl Cyclohexyl*)-18-*Crown*-6 (*XXXII*)

Our initial studies were concerned with the cyclic polyether bis cyclohexyl-18-Crown-6, which is diagrammed in Fig. 5 and referred to hereunder as XXXI, following Pedersen's (1967) terminology. We found that although the qualitative effects of this polyether on bilayers

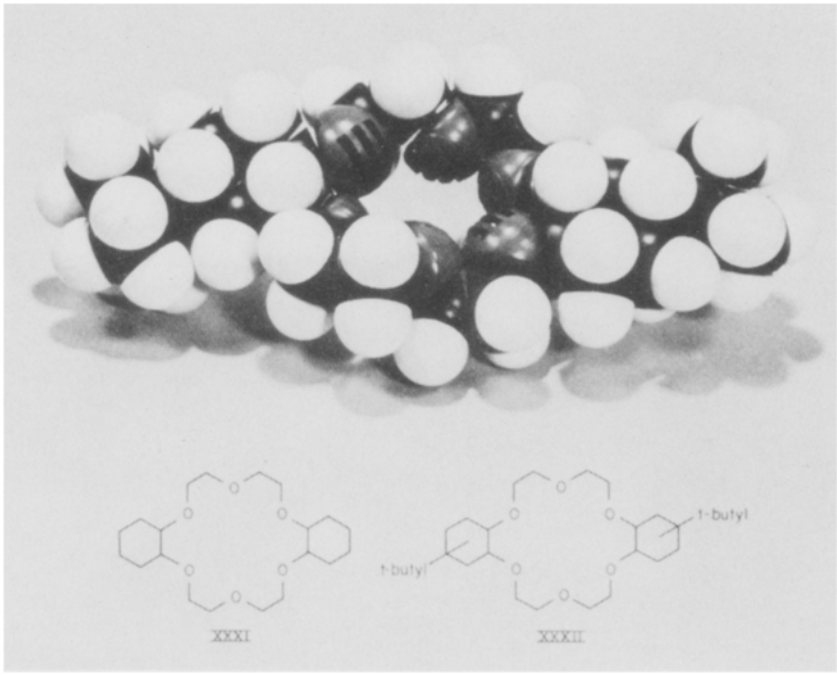

Figure 5. Chemical formulae for the cyclic polyethers XXXI (left) and XXXII (right). CPK Model of XXXII above.

and on salt extraction equilibria resembled those of the macrotetralide actins, there were serious quantitative discrepancies between the experimental observations and the theoretical expectations (Eisenman *et al.*, 1968). Specifically, for valinomycin and the macrotetralide actins, the ratios P_i/P_j, G_i/G_j and K_i/K_j were the same for a given pair of cations, whereas for the polyether the permeability and conductance

ratios not only disagreed with each other, but also with the salt extraction equilibrium data.*

We have been able to resolve these apparent discrepancies by extending our studies to the more lipid soluble t-butylated analog of XXXI, bis(t-butyl cyclohexyl)-18-Crown-6, diagrammed in Fig. 5 and abbreviated hereunder as XXXII. The resolution of these apparent discrepancies involves only a direct extension of the previous theoretical

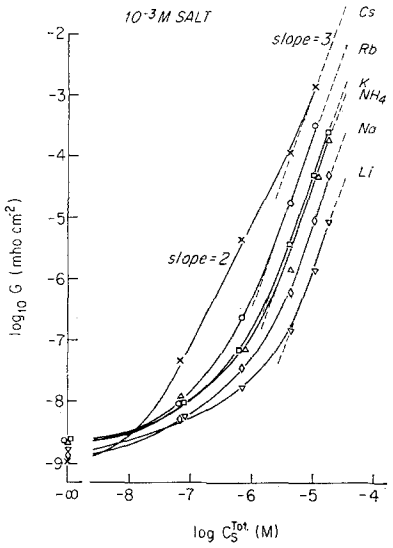

Figure 6. Dependence of membrane conductance on the aqueous concentration of polyether XXXII in the presence of 10^{-3} M chloride solutions of the indicated cations. The ordinate plots the logarithm of the observed membrane conductance; while the abscissa plots the logarithm of the total concentration of the polyether in the aqueous solution. The dashed lines are drawn with a slope of 3; while the slope of the Cs conductance between 10^{-7} and 10^{-6} M is 2. Asolectin membrane.

analysis of the carrier model to include the possibility that the polyethers form 2:1 and 3:1 carrier-cation complexes in the membrane. Such an extended theory predicts novel phenomena such as the presence of a maximum in the membrane conductance with increasing permeant ion concentration (when the ionic strength is maintained constant with an "indifferent" electrolyte) and variations in the cationic conductance sequences with salt concentrations. It enables us also to calculate the formation constants of 1:1 polyether-cation complexes in the aqueous solution for comparison with those measured directly. Since a detailed theoretical and experimental analysis has been submitted for publication elsewhere (McLaughlin, Szabo,

* The permeability ratios for XXXI were in the sequence K > Rb > Cs > Na > Li, whereas the conductance ratios were in the sequence Cs > Rb > K > Na > Li and the salt extraction sequence was K > Rb > Na > Cs > Li.

Ciani and Eisenman, 1972), only the main experimental features will be presented here.

The effects of the polyether XXXII on the membrane conductance and potential are illustrated in Figs. 6 and 7, respectively, for bilayers formed from asolectin. Fig. 6 shows the dependence of membrane conductance on the aqueous concentration of polyether in the presence of 10^{-3} M chloride solutions of the indicated cations. Comparison of the data of Fig. 6 with the previous findings for XXXI (Eisenman *et al.*,

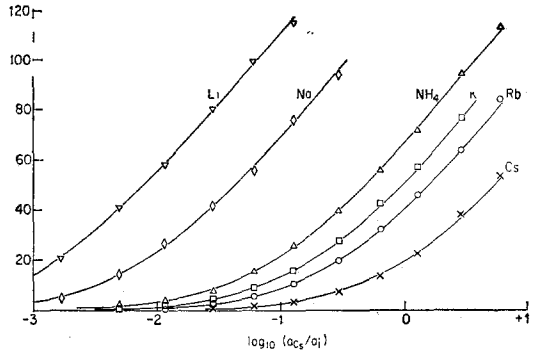

Figure 7. Membrane potentials in mixtures of cesium nitrate with the indicated alkali metal chlorides. The ordinate plots the observed values of the steady-state potential differences between the solutions on the two sides of the membrane; while the abscissa plots the logarithm of the ratio of the activity of the cesium ion to the activity of the indicated cation. The experiment was carried out in the same manner as Fig. 4 of Szabo *et al.*, 1969 by adding small volumes of cesium nitrate to one side of a membrane bathed initially on both sides in 10^{-3} M chlorides of the indicated cations. The points are experimentally measured; while the curves are drawn according to the theoretical expectations of equation 1 for the following values of permeability ratios: P_{Rb}/P_{Cs} (0·25), P_K/P_{Cs} (0·15), P_{NH_4}/P_{Cs} (0·075), P_{Na}/P_{Cs} (0·0070), and P_{Li}/P_{Cs} (0·0013). Asolectin membrane.

1968, Fig. 6c) shows that XXXII has a markedly greater ability to enhance the membrane conductance than does XXXI. This confirms John Rowell's original finding (personal communication, 1969) of the higher potency of XXXII than XXXI on bilayers. (The comparative effects of these two molecules will be discussed further in relation to Fig. 12). The conductances in a 10^{-3} M salt solution are seen to decrease in the sequence: $Cs > Rb > K > NH_4 > Na > Li$, identical to the sequence previously observed for XXXI (Eisenman *et al.*, 1968; Fig. 15).*

Figure 7 illustrates the corresponding effects on the membrane potential in the presence of 10^{-5} M XXXII (the points are the experi-

* The ability of XXXII to produce a very high Cs^+ conductance in bilayers has practical implications for using this molecule as a "probe" for examining cell membranes. For example, whereas it is difficult to detect an additional conductance when adding valinomycin or a macrotetralide to a squid axon (Gilbert *et al.*, 1970), presumably because of the intrinsically high K^+ conductance of this axon, it should be possible to detect the additional Cs^+ conductance for XXXII because of the low conductance characteristic of the squid axon in Cs^+ solutions (Baker *et al.*, 1962; Adelman and Fok, 1964).

mentally observed potentials; the curves are drawn from the theoretical equation (1) with the permeability ratios indicated on the figure). Note that equation (1) describes the experimental observations perfectly and that the observed Nernst slope implies the membrane is ideally permselective to cations in the presence of this polyether. It is important to note that the relative permeabilities to the various cations are in the same sequence as were the conductances, $Cs > Rb > K > NH_4 > Na > Li$. The close correspondence between the permeability and conductance ratios for the various cations from these two sets of data can best be compared in Table IV, where the data from Figs. 6

TABLE IV. Identity between conductance ratios and permeability ratios for the polyether XXXII at 0·001 M salt concentration

	$G^0(I)/G^0(Cs)$	P_i/P_{Cs}
Cs	1·00	1·00
Rb	0·20	0·25
K	0·044	0·15
NH_4	0·035	0·075
Na	0·0077	0·007
Li	0·0013	0·0013

and 7 are summarized. This correspondence verifies for XXXII the important identity of equation (14) and indicates that there is no discrepancy between permeability and conductance ratios for this polyether. (The reasons for the different permeability sequences observed with XXXI and XXXII will be considered at the end of this section).

Despite the general similarities between the observations so far described for XXXII and for the macrotetralides and valinomycin, certain important differences are apparent on examining Fig. 6 in greater detail. For the macrotetralides and valinomycin the membrane conductance was proportional to the first power of the antibiotic concentration, whereas the data of Fig. 6 indicate a second power dependence for cesium on polyether concentration in the region around 10^{-6} M and a third power dependence for all cations at the highest polyether concentrations. The data of Fig. 6 (see also Fig. 12), together with the observation that the membrane conductance at constant ionic strength is proportional to the first power of permeant cation concentration (at low salt concentration, as can be seen clearly for cesium in Fig. 11), strongly suggest the existence of a complex in which more

than one cyclic polyether is needed to solubilize the cation in the membrane. It is seen in Fig. 6, and will become further apparent in Fig. 12, that there is a region where the 2:1 complex of Rb^+ and Cs^+ appears

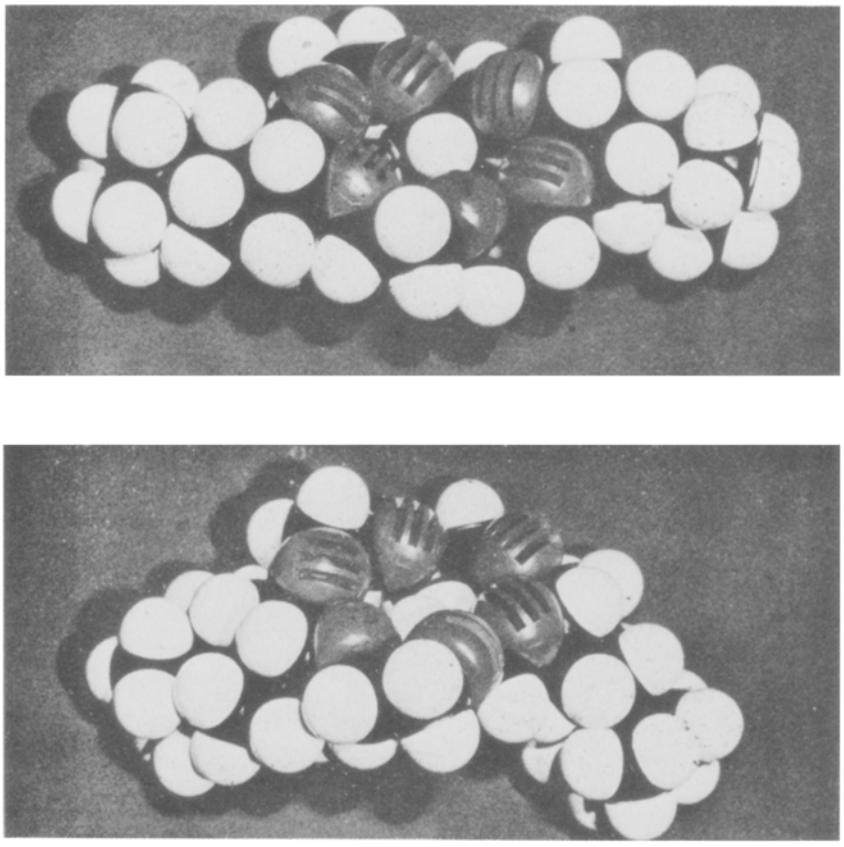

Figure 8. Two conceivable configurations for the cyclic polyether, XXXII. Top, twisted along the long axis; bottom, bent along the long axis. The 2 to 1 complex can be envisaged as sandwiching a cation between two molecules in the "planar" configurations of Fig. 5; while the 3 to 1 complex could be formed from the bottom or top configurations as a propeller-shaped, or sausage-shape complex around a cation; having an hydrophobic exterior and polar interior.

to be the permeant species; while at the highest polyether concentrations, the permeant species for all cations appears to be the 3:1 complex.* Thus, a principal difference between the cyclic polyether XXXII and the macrotetralides (as well as valinomycin) is the necessity for more than one polyether molecule to be utilized in solubilizing the

* This cubic dependence of conductance on polyether concentration is not restricted to asolectin membranes, but is also characteristic of bilayers formed from the phospholipids DC, PE and PG, as can be seen in Fig. 1 of McLaughlin *et al.*, 1970.

cation within the membrane.* The 2:1 complex is possibly a sandwich, with Cs and Rb constituting the filling, for these ions are too large to fit into the cavity of a single polyether molecule (Bright and Truter, 1970), and evidence exists for such a complex (Pedersen, 1970). The nature of the proposed 3:1 complex is unknown, but the polyether molecule can be deformed in at least two different ways, as illustrated in Fig. 8, and there are several possible ways that three such deformed molecules could arrange themselves around the cation.

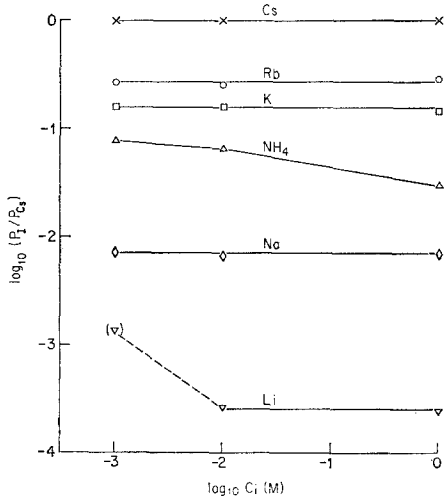

Figure 9. Constancy of permeability ratios at various salt concentrations. The permeability ratios were measured at 10^{-5} M polyether concentration as in Fig. 7 by adding $CsNO_3$ to the alkali metal chlorides at the indicated initial concentrations. Asolectin membranes.

The permeability ratios for XXXII are independent of salt concentration, as was also found to be the case with the macrotetralides and valinomycin. This is illustrated in Fig. 9, which presents the permeability ratios as a function of salt concentration (measured as in Fig. 7) for 10^{-3}, 10^{-2}, and 1 M salt concentration levels and for a 10^{-5} M concentration of polyether. The apparent variation in the lithium permeability at the lowest concentration is probably an artifact due to the presence of a low concentration of contaminants such as NH_4^+ and H^+; whereas the concentration dependence for NH_4^+ is small but real. This concentration independence of the permeability ratios is expected even when there is a significant degree (cf. Frensdorff, 1971) of complex formation in the aqueous solution.†

* Although a search for the existence of 3:1 complexes with the alkali metal cations has not been made in hydrocarbon solvents comparable to the interior of the bilayer membrane, the existence of higher complexes of polyethers with the alkali metal cations is becoming increasingly recognized (Bright and Truter, 1970; Frensdorff, 1971).

† The permeability ratios will be independent of salt concentration if the diffusion of the polyether molecules through the membrane is rapid compared to its rate of diffusing through

The conductance ratios for the polyether, however, depend markedly on the salt concentration. This can be seen clearly in the data of Fig. 10, which summarizes, for a 10^{-5} M concentration of polyether, the conductance observations from Fig. 6, together with conductances measured at higher salt concentrations. It is apparent from Fig. 10 that although the sequence of conductance ratios is the same as that of the

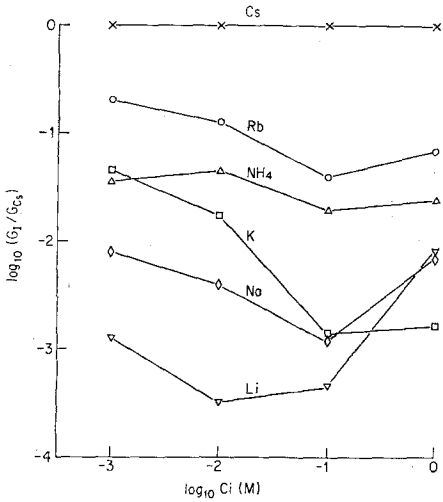

Figure 10. Dependence of conductance ratios on salt concentration. This figure summarizes the dependence of observed membrane conductances at 10^{-5} M polyether concentration from Fig. 6 and similarly obtained measurements at higher salt concentrations. Note that, in contrast to the permeability ratios, the conductance ratios depend markedly on salt concentration. Asolectin membranes.

permeability ratios at 10^{-3} M salt concentrations, the sequence differs at 10^{-2} M by inversion of the potassium and ammonium conductances. This inversion is more pronounced in the 1 M salt solution, where the conductances of lithium and sodium have both crossed potassium, so that the conductance sequence is now Cs > Rb > NH_4 > Li > Na > K. It will be shown below that these apparent complexities are a consequence of the cubic dependence of conductance on polyether concentration and the existence of significant quantities of 1:1 complexes in the aqueous solutions. Notice that the data of Figs. 9 and 10 have been obtained at 10^{-5} M polyether concentration, a concentration where the conductance depends on the cube of the carrier concentration for all cation species. This is necessary in order to simplify the treatment.

the unstirred layers or crossing the interfaces on either side of the membrane (cf. Szabo *et al.*, 1970, Case B, equations. (36)–(38)). A complete analysis of this problem has been carried out for XXXII (McLaughlin *et al.*, 1972) and it has also been verified experimentally that the rate limiting step for the movement of the neutral polyether is in fact diffusion through the aqueous unstirred layers.

We have deduced (McLaughlin, Szabo, Eisenman and Ciani, 1972) from a theoretical analysis of a carrier model that, when essentially only 3:1 complexes exist in the membrane phase and 1:1 complexes in the aqueous phase, the conductance and permeability ratios should be interrelated by:

$$\frac{G_0(\mathrm{J})}{G_0(\mathrm{I})} \cdot \frac{P_i}{P_j} = \frac{(1 + K_{is}^{+} a_i)^3}{(1 + K_{js}^{+} a_j)^3} \tag{19}$$

instead of the simpler identity of equation (14). Moreover, the conductance is defined by the more general equation (20) instead of equation (3).

$$G_0 = \frac{F^2}{d} u_{is_3}^{*} k_{is_3} K_{is_3}^{+} \frac{(C_s^{\mathrm{Tot}})^3}{(1 + K_{is}^{+} a_i)^3} \cdot a_i \tag{20}$$

In these equations, K_{is}^{+} and K_{js}^{+} are the stability constants for the formation of the 1:1 complexes in water, as before, but the subscripts "is_3" refer to the 3:1 complex. Note that the term $C_s^{\mathrm{Tot}}/(1 + K_{is}^{+} a_i)$ in equation (20) is merely the free concentration of the polyether in the aqueous phase and that the product of the last three terms is, as before, the concentration of the permeant charged complex in the aqueous phase.

Equation (19) predicts that the permeability and conductance ratios should differ if significant complex formation occurs in the aqueous phase with formation constants K_{is}^{+} and K_{js}^{+}. In the limit of sufficiently low salt concentration, however (i.e. when the product $K_{is}^{+} a_i \ll 1$), the conductance and permeability ratios are expected to be identical, as indeed was observed in 10^{-3} M salt solutions (Table IV). At higher salt concentrations, it is possible to calculate values for the formation constants, K_{is}^{+}, from equation (19) by comparing the ratios of conductance and permeability at a given salt concentration. If we take species J to be lithium, and assume that its association with polyether is negligible in 10^{-2} M salt solutions (i.e. $K_{\mathrm{Lis}} \cdot 10^{-2} \ll 1$) then equation (19) reduces to the simple form

$$(1 + K_{is}^{+} a_i)^3 = \frac{G_0(\mathrm{Li})}{G_0(\mathrm{I})} \cdot \frac{P_i}{P_{\mathrm{Li}}} \tag{21}$$

The values of K_{is}^{+} calculated from the conductance and permeability data obtained in 10^{-2} M salt solutions by using equation (21) are given in the first column of Table V. These may be compared with values obtained for the two isomers, A and B, of XXXI (XXXII is too insoluble in water for measurements to be made on it) obtained by Frensdorff (1971) using glass electrodes and by Izatt, Nelson, Rytting, Haymore and Christensen (1971) using a calorimetric technique. The agreement in Table V is remarkably satisfactory, both as to sequence and to the magnitude of the values observed for the aqueous 1:1 complex formation constants, K_{is}^{+}.

TABLE V. Comparison of values of aqueous complex formation constants deduced from our bilayer membrane measurements for XXXII with those directly measured for XXXI

	Membrane* (potential vs. conductance)	Frensdorff† (glass electrode)		Izatt *et al.*‡ (calorimetric)	
	XXXII	XXXIA	XXXIB	XXXIA	XXXIB
K	120	150	60	100	40
Rb	34	—	—	31	4
Na	26	50	30	—	—
NH_4	19	27	6·5	22	16
Cs	12	18	7	13	—
Li	<4	5	—	—	—

All values are in liters per mole.
* Comparison between permeability ratios and conductance ratios in 0·01 M salt.
† Measurements for the two different isomers A and B by Frensdorff (1971) using cation selective glass electrodes.
‡ Calorimetric measurements by Izatt *et al.*, 1971.

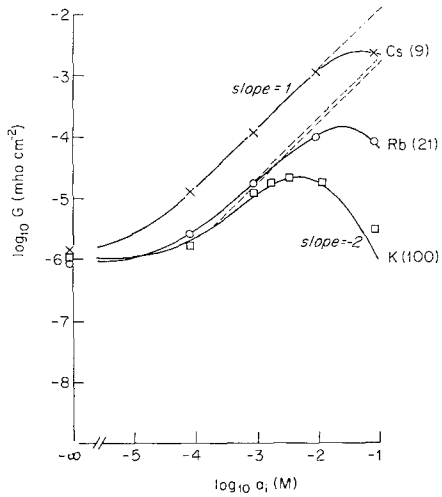

Figure 11. Dependence of membrane conductance on salt concentration at constant ionic strength. The ordinate plots the observed values of membrane conductance, while the abscissa plots the activity of indicated cation in solutions whose ionic strength was maintained constant at 0·1 M with LiCl. The points are experimental measurements; while the curves are drawn theoretically according to equation (20) for the following values of K_{is}^{+}: Cs (9), Rb (21), K (100). The dashed lines are drawn with a slope of 1. Asolectin membranes.

A further test of the present model becomes apparent on examination of equation (20). This equation predicts that the membrane conductance should first increase linearly (when $K_{is}^{+}a_i \ll 1$) with the concentration of permeant cation, a_i, should then go through a maximum (when $K_{is}^{+}a_i = 0{\cdot}5$) and then should ultimately decrease with an inverse square dependence on a_i (when $K_{is}^{+}a_i \gg 1$). This is in fact the

observed behavior of the system, as is illustrated in Fig. 11. The data in Fig. 11 were obtained under conditions in which the ionic strength was held constant with the relatively impermeant or "indifferent" electrolyte, lithium chloride. The observed conductance data are plotted as points while the solid curves have been drawn according to equation (20) using the indicated values of the aqueous association constant, K_{is}^{+} (which are in a close agreement with those in Table V).

Comparison of the Properties of Polyethers XXXII and XXXI

We turn now to a comparison of the effects of XXXI and XXXII in order to reconcile the last remaining discrepancy between permeability and conductance ratios observed for XXXI, which was mentioned in the introduction to this section. The effects of the polyethers XXXI and XXXII on bilayer membranes are best compared in Fig. 12, which illustrates the dependence of membrane conductance on

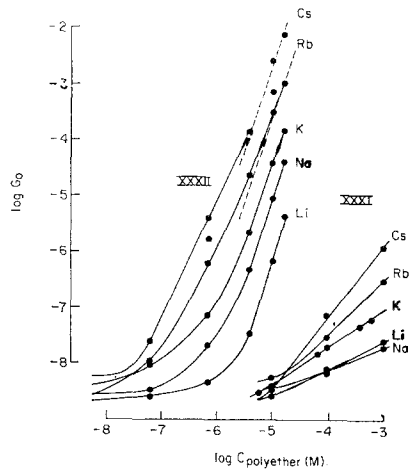

Figure 12. Comparison of the effects of polyethers XXXI and XXXII on membrane conductance. The logarithm of the membrane conductance for asolectin membranes is plotted as a function of the logarithm of the total polyether concentration at 0·1 M concentration of the indicated cations. The principal difference between the two polyethers is that XXXII is about 1000 times more effective than XXXI, in accord with their measured partition coefficients between water and hexane.

XXXI and XXXII concentrations under identical conditions. It is apparent from Fig. 12 that the effects of these polyethers on the membrane conductance are qualitatively similar. The conductance ratios for both of the polyethers are in the same lyotropic sequence. The main difference is that the tertiary butylated polyether XXXII is about a thousand times more effective than XXXI.*

* The principal effect of tertiary butylation on the polyethers is presumably to increase its membrane partition coefficient without markedly effecting its energy of interaction with the cations. Indeed, the partition coefficient of XXXII between water and hexane has been shown to be about 10^4 in favor of hexane, a factor of a thousand greater than the partition coefficient of XXXI into hexane (McLaughlin *et al.*, 1972).

Why, then, do permeability and conductance ratios previously noted for the cyclic polyether XXXI (Eisenman *et al.*, 1968) differ from one another or, alternatively, why are the permeability ratios for XXXI and XXXII different? The reason for this can be seen from the data presented in Fig. 13, where it is apparent that the Cs/K permeability ratio for XXXII is constant only when the polyether concentration in the solution exceeds 10^{-6} M. Below this concentration the

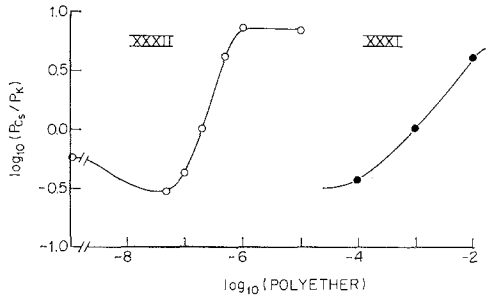

Figure 13. Dependence of permeability ratios on polyether concentration at very low (membrane) concentrations of polyether. This figure illustrates that the permeability ratio P_{Cs}/P_K is independent of XXXII concentration only above 10^{-6} M polyether; below this concentration, this permeability ratio depends on polyether concentrations. Note that all measurements of Figs. 8, 10, 11 and 13 were made at 10^{-5} M polyether. The right-hand portion of the figure illustrates a similar dependence of permeability ratio for XXXI, which naturally occurs at much higher polyether concentrations because of lower partition coefficient of XXXI than XXXII. See text for further details. Asolectin membranes.

permeability ratio, P_{Cs}/P_K, decreases and inverts, so that at low polyether concentrations the membrane is more permeable to potassium than to cesium. This phenomenon is also present for XXXI, as can be seen in the right-hand portion of Fig. 13. For the less favorably partitioned molecule, XXXI, however, we have had to increase the polyether concentration considerably above that in our previous publication in order to produce the change in the permeability ratios. Once the membrane concentrations of the two polyethers are scaled in terms of their different partition coefficients, the phenomena are seen to be remarkably comparable. Below a certain polyether concentration (i.e. about 10^{-6} M for XXXII and about 10^{-2} M for XXXI), the permeability ratios are a function of the polyether concentration (and different from the conductance ratios over a certain range), because of a combination of two effects described briefly below.*

* The phenomena illustrated in Fig. 13 presumably arise because at low polyether concentrations the most permeant species is the 1:1 complex. As the association constant for the 1:1 complex in water is greater for K than for Cs (see Table V), and therefore so should be the value of $\bar{K}_i$ for solubilizing the 1:1 K^+ complex in the membrane, it is reasonable that the membrane is more permeable to K than Cs at the lowest polyether concentrations. The inversion of the permeability ratio, P_{Cs}/P_K, occurs before the inversion of the conductance ratio, G_{Cs}/G_K, because a secondary effect of complex formation in the aqueous phase is to reduce the free polyether concentration. Permeability and conductance ratios are compared

We conclude that the behavior of XXXI is similar to that of XXXII and that the main difference between these two molecules is that XXXII has a partition coefficient about a 1000 times greater than that of XXXI. The effects that both these molecules produce on the permeability and conductance properties of bilayer membranes may be understood in terms of the present simple theoretical framework once it is recognized that a significant degree of association occurs in the aqueous phase and that at higher polyether concentrations the permeant species are no longer the simple 1:1 complexes as was the case for valinomycin and the macrotetralide antibiotics.

Quantitative Comparison of the Cation Selectivity of Valinomycin and the Macrotetralides with that of Biological Membranes

This section compares the cation selectivities characteristic of the macrotetralide actins and valinomycin with each other, as well as with the selectivities characteristic of biological membranes. It demonstrates that the quantitative pattern of selectivity among the alkali metal cations for the macrotetralide actins is distinguishable in certain important features from that characteristic of valinomycin. Moreover, the macrotetralide pattern is quite different from the pattern for cell membranes. By contrast, the quantitative selectivity of valinomycin for Li^+, Na^+, K^+, Rb^+ and Cs^+ is surprisingly close to that characteristic of the membranes of living cells. A further similarity between the data for the cell membrane and valinomycin (and a further difference between the cell membrane and the macrotetralide actins) comes from the selectivity for NH_4^+ which is similar for valinomycin and for the cell membrane, but is markedly different for the macrotetralide actins.

The rationale underlying the comparison to be presented here is that quantitative differences in selectivity are expected between molecules having different types, numbers, and orientations of the cation-binding ligands; and such differences may be useful as "fingerprints" for comparing the observed selectivity pattern in an unknown system with that characteristic of well defined molecules of known ligand type and configuration. Indeed, empirically generated selectivity patterns have been described for such diverse systems as glass electrodes (Eisenman, 1962) and cell membranes (Eisenman, 1963, 1965), which differ in important quantitative details. (Compare Figs. 15 and 16). For glass these have proven useful in systematizing the effects of a wide variety of cations on electrodes of diverse composition. In particular, it has been found possible to predict successfully the relative permeabilities of the species Li^+, Rb^+, Cs^+, NH_4^+, Ag^+, Tl^+ solely from a knowledge of

at the same total concentration of polyether, but the free concentration in the membrane for the P_K/P_{Cs} measurement is lower than that for the Cs conductance measurement and higher than that for the K conductance measurement, as is discussed in more detail elsewhere (McLaughlin *et al.*, 1972).

the P_{Na}/P_K ratio (Eisenman, 1967, cf. Figs. 4–7 of Chapter 9). For the moment, we ask the reader to bear with us in accepting the postulate that it will be instructive to compare the quantitative selectivities empirically observed for valinomycin and the macrotetralide actins to see whether or not we can identify distinguishable differences in the way these molecules select among cations for comparison with the selectivity "fingerprints" characteristic of cell membranes.

To define what we mean by an empirical selectivity pattern, let us begin with the selectivity among certain monovalent cations characteristic of glass electrodes. Figure 14 (which reproduces Fig. 9–4 of Eisenman, 1967) demonstrates the experimental evidence for the existence of a quantitative pattern of relative selectivities among the cations Li^+, Na^+, K^+, Rb^+, Cs^+, and H^+ for alumino-silicate glass electrodes, as well as air-dried collodion membranes. The ordinate plots the experimentally observed membrane potential differences, relative to K^+, for the various cations at pH 7 in 0·1 normal solutions. These values correspond to $58 \log P_i/P_K$ in present terminology. The effects of the individual cations relative to K^+ are indicated on each of the subfigures. Thus, the uppermost subfigure gives the permeability ratios of Li^+ relative to K^+. All data points below the horizontal line symbolizing K^+ represent glass compositions for which Li^+ was found to be more permeable; whereas all data points above the horizontal line represent glasses for which K^+ is more permeable. Data points at the same location on the abscissa of all subfigures represent observations for a given electrode composition. Over all of the figure except the extreme right-hand portion, the relative effects of cations for differing compositions of glasses have been ranked using the observed permeability ratio of Na^+ vs. K^+. This has been done by locating each composition from left to right by putting its point on the Na^+ "isotherm". Notice that the points must lie exactly on the straight line, since this has been chosen arbitrarily to define a left to right position for a given composition. Once this position is fixed for a given composition, the permeability ratios for the other cations are plotted according to their observed values on each of the subfigures. When this has been done, it becomes apparent that the data for each of the cations are described by the rather simple lines, henceforth called "isotherms", drawn on the figure as visual averages of the experimental points. Such simplicity need not have been the case. In this way, a set of isotherms was characterized for sodium alumino silicate glass electrodes (Eisenman, 1962) and subsequently found to apply also to collodion membranes and electrodes in which the original sodium oxide of the composition was replaced by other alkali metal oxides. The range of membrane compositions is indicated by the designations "LAS", "NAS", at the lower right of Fig. 14, which indicate lithium alumino silicate, sodium alumino silicate, etc. compositions. The isotherms from Fig. 14 could

then be superposed into a set giving an overall selectivity pattern as has been done in Fig. 15. It is this sort of pattern with which we will be dealing in the remainder of this section; but before concluding this

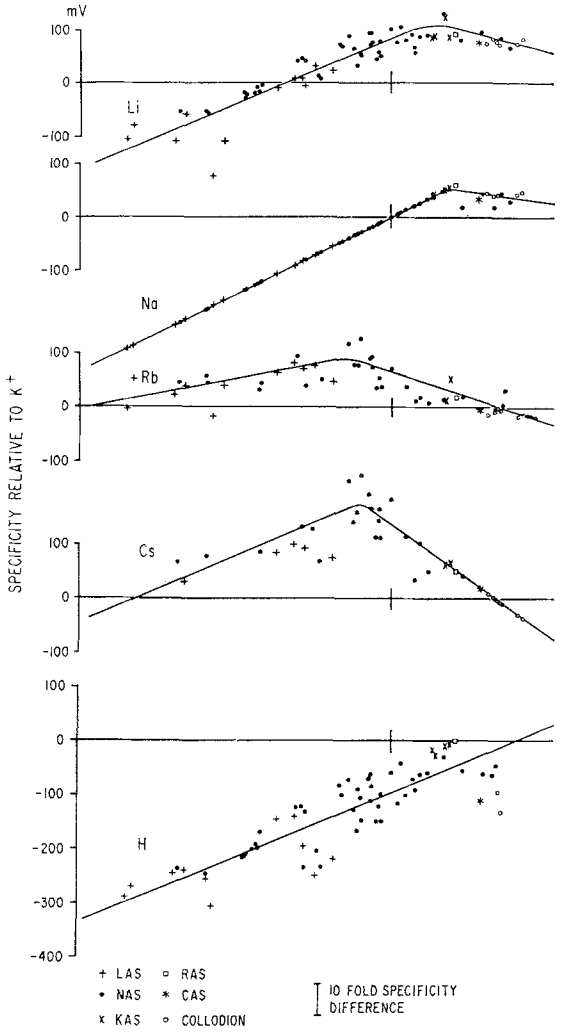

Figure 14. Experimental evidence for the existence of a quantitative pattern of cation selectivity for glass electrodes and collodion membranes. (After Fig. 9–4 of Eisenman, 1967). The membrane potential differences are indicated in millivolts (58 mV corresponds to a 10-fold selectivity difference). Data points for the indicated compositions are given by the symbols below the figure. See text for full details.

section it should be pointed out that this, entirely empirically developed, quantitative pattern has proven useful not only in describing a vast amount of data on electrodes of diverse composition but also in predicting for new compositions the relative effects of a wide variety of

cations from a simple knowledge of the P_{Na}/P_K ratio. It should be apparent that *a knowledge of this ratio alone allows the permeability ratios relative to potassium for the other cations to be predicted through the selectivity pattern of Fig.* 15.*

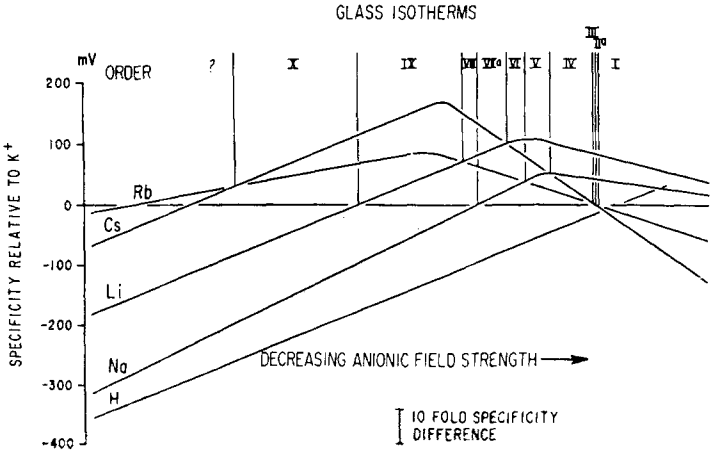

Figure 15. Selectivity pattern for glass and collodion membranes. The isotherms of Fig. 14 have been superposed to yield the selectivity pattern indicated here.

Let us now turn to comparable considerations for cell membranes. An examination of data in the literature for the permeation, accumulation, enzyme activation, and electrogenic action of Li^+, Na^+, K^+, Rb^+ and Cs^+ has indicated that these ions differ only quantitatively, and the empirical specificity pattern shown in figure 16 was proposed

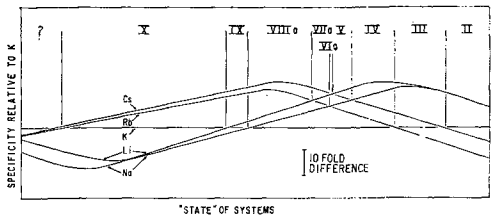

Figure 16. Biological selectivity pattern (after Figs. 8 and 9 of Eisenman, 1965). Details of the manner in which this figure was constructed are given elsewhere (Eisenman, 1965), and will be considered explicitly for cell membrane potential data in Fig. 17.

to describe these differences in biological phenomena (Eisenman, 1963). The generality of this pattern and its usefulness has received further support in more recent work (Eisenman, 1965) and from findings of analogous patterns for anions and divalent cations in biological systems

* It goes beyond the scope of the present section to discuss the fact that the Na^+ isotherm is not simply a straight line but shows a maximum at the right. In this case the data have had to be scaled by the extrapolated Cs^+ isotherm. This is a small degree of degeneracy in the data, which is discussed elsewhere (Eisenman, 1962, 1967).

by Diamond and Wright (1969).* Figure 16 presents the set of isotherms extracted in the same manner as Fig. 14 from a wide variety of biological selectivity data in the literature. Ordering the data according to the relative effects of a given pair of cations (Rb^+ and K^+ were used for convenience), it was found that the effects of the other alkali metal cations could be systematized. As for glasses, this need not have been the case. The essential feature of the "biological selectivity pattern" is that *specifying the selectivity for a given pair of cations allows one to determine quantitatively the selectivity for the other three alkali metal cations*. Even though such a correlation is empirical, and its usefulness is quite independent of any theoretical arguments, it should be noted that the existence of such a selectivity pattern is suggested from considerations of the balance of energies between ion-site vs. ion-water interactions, as examined in the last section.

The biological selectivity pattern of Fig. 16 requires that a given permeability ratio between any two cations (e.g. P_{Na}/P_K) specify a particular set of permeability ratios for all the other cations. The extent to which this is verified for cell membranes will now be critically examined in order to provide a basis for comparison with the present antibiotics. Figure 17 plots as data points the observed cationic permeability ratios (relative to K^+) for various physiological states of the nerve membrane and compares these with the solid curves which represent the postulated biological specificity isotherms of Fig. 16. (Note that these curves were deduced from a large variety of independent data.)

The ordinate plots the permeability ratio of the indicated cations (symbolized by I^+) relative to K^+. Data points for each of the cations have been located from left to right along the abscissa using the observed P_{Na}/P_K values to rank each set of observations from varying physiological "states" of the axon along the straight line segment of the Na isotherm. This uniquely locates the observed permeabilities to the other cations along the x-axis. For example, consider the set of data points labelled "18-underswing" on Fig. 17. These data represent the relative permeabilities calculated from the effects of Rb^+, Cs^+, Na^+ and K^+ on the membrane potential of the squid axon during the post-spike underswing (Baker, Hodgkin and Shaw, 1962). In their experiments the ratio P_{Na}/P_K was measured to be 0·03, the effect of 10 mM Rb^+ was found to be indistinguishable from that of 10 mM K^+, and 10 mM Cs^+ had the same effect in reducing the underswing as 3 mM K^+. From these data the appropriate permeability ratios for Rb and Cs were calculated to be: $P_{Rb}/P_K = 1$, $P_{Cs}/P_K = 0{\cdot}33$. There is only one

* It should be apparent that, although Figs. 15 and 16 exhibit sequences of cation selectivities which are qualitatively similar, the two patterns are easily distinguishable in many quantitative details. We propose to make use of this type of distinction below when we extend the comparison of empirically observed quantitative selectivity behavior to the macrotetralide actins vs. valinomycin.

place on the straight line segment of the Na^+ isotherm of Fig. 17 to locate P_{Na}/P_K, namely at the point indicated by the half filled dot. Therefore the data for Rb^+ and Cs^+, must also be located at this position along the abscissa. Notice that the Rb^+ data point corresponds precisely to the expected position of the Rb^+ isotherm here, while the Cs^+ data point corresponds quite closely to that of the Cs^+ isotherm. In the same way all of the other data points were plotted on Fig. 17.

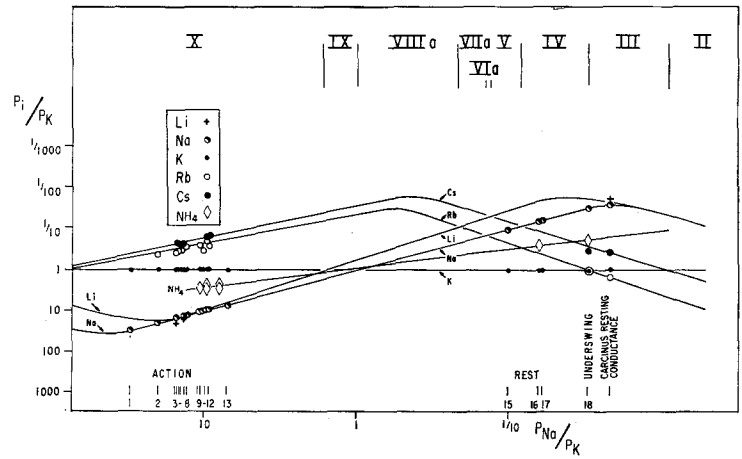

Figure 17. Selectivity pattern for cell membranes. The curves representing the empirical biological specificity isotherms of Fig. 16 are compared with the permeability ratios in various physiological states of the squid giant axon membrane, as well as the resting membrane conductance of Carcinus nerve. Data points represent observations for the permeability ratios of the indicated cations in varying physiological "states" of the axon, scaled along the abscissa by the observed P_{Na}/P_K values as described in the text using the biological Na^+ vs. K^+ selectivity isotherm (a straight line over the range of these data).

From left to right, the data come from the following sources: The points above numbers 1 and 13 represent P_{Na}/P_K measured by Baker, Hodgkin and Shaw (1962); numbers 2 through 12 are permeability measurements from individual experiments of Chandler and Meves (1964). Numbers 15 and 16 are the externally measured resting P_K/P_{Na} values of Baker, Hodgkin and Shaw (1962); while number 17 is the resting P_K/P_{Na} ratio measured by Adelman and Fok (1964). Number 18 represents the relative permeabilities in the underswing state reported by Baker, Hodgkin and Shaw (1962). In addition to these permeability ratios, Fig. 17 includes membrane conductance ratios (labelled "CRC") deduced from Hodgkin's (1947) data for *Carcinus Maenas* nerve.*

* The reason for the correspondence of conductance ratios and permeability ratios, an expectation of the independence principle, is seen intuitively from equation (14). The fact that the conductance ratios agree so well with the extrapolated expectations for the permeability ratios, albeit from different axons, is an interesting, although possibly coincidental, feature in which certain cell membranes resemble bilayer membranes treated with the present antibiotics. A further discussion of the independence principle will be found in Ciani *et al.*, 1969.

Also included in Fig. 17 are data for NH_4^+ from the recent studies of Binstock and Lecar (1969). These authors have characterized the effects of NH_4^+ on the early transient current, as well as the delayed currents, in voltage clamp studies on perfused squid giant axons. For the action potential region, Binstock and Lecar's P_{NH_4}/P_{Na} values (indicated by the diamond shaped symbol) for individual axons have been located from left to right by their observed values of P_K/P_{Na}. Although these authors did not report values for P_{Na}/P_K in the resting and underswing states of the axon, they did find P_{NH_4}/P_K to be 0·26 for the resting potential and P_{NH_4}/P_K to be 0·2 for the underswing potential. These permeability ratios for NH_4^+ have therefore been located in the resting region and underswing region, respectively by the P_K/P_{Na} ratios corresponding to these states on this figure. The NH_4^+ permeability data are seen to lie on the straight line labelled "NH_4^+" on the figure, which we will tentatively take as the ammonium isotherm for the cell membrane for comparison with the NH_4^+ data for the macrotetralide actins and valinomycin.

Note the remarkably close correspondence between the observed data points and the particular isotherms for each of the alkali metal cations, as well as for NH_4. At the very least the data of Fig. 17, therefore, indicate that a given permeability ratio observed between any two cations (e.g. P_{Na}/P_K) implies a particular set of selectivities for all the other cations. This is expected if a particular set of selectivities reflects a particular spatial array of ligand oxygens of a particular molecule.* The observed differences of selectivity from one cation to another are then a consequence of their different energies of interaction with these molecules (in competition with their energies of hydration), as examined in the last section. The empirical patterns can be likened to "fingerprints" for the detailed interactions between cations and the ion binding molecules, and comparison of the quantitative selectivity pattern for molecules with known (or at least knowable) configurations of ligand oxygens is then instructive in terms of attempting to deduce something about the intimate nature of cation-ligand interaction in the unknown biological membrane. It is to this that we now turn our attention.

Figures 18 and 19 present selectivity data for the macrotetralide actins and valinomycin for comparison with the cell membrane selectivity pattern. The observed data for the macrotetralide actins are indicated in Fig. 18 by points (K_i/K_K values on the left side, P_i/P_K values on the right side), and the biological isotherms of Fig. 17 have been indicated by fine lines for comparison. In both portions of the figure, the average selectivities for the macrotetralide actins, taken from

* A pattern could then develop from a set of selectivities of a given array by small perturbations of dipole moment of the ligand oxygens as, for example, is seen from the effect of adding the electron-withdrawing methyl groups to the members of the macrotetralide actin series of antibiotics (Eisenman *et al.*, 1969).

the more accurate salt extraction data are indicated by the heavy lines. Notice the large differences (indicated by the arrows) between the selectivities induced by these molecules and the biological selectivity isotherms. Clearly, there is *not* a quantitative correspondence between the pattern of selectivity observed for the macrotetralide actins and the pattern of selectivity for the cell membrane, the differences for the ammonium ion being the most striking.*

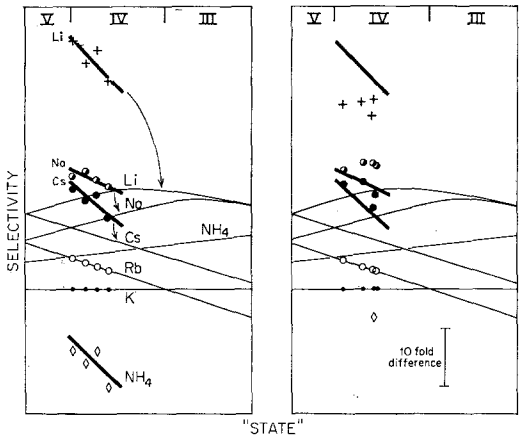

Figure 18. Comparison of the selectivity data for the macrotetralide actins with the selectivity pattern for cell membranes. Salt extraction equilibrium data (left) and permeability ratios (right) have been scaled along the abscissa according to K_{Rb}/K_K and P_{Rb}/P_K, respectively. Notice that there are marked differences between the observed cation selectivities for the macrotetralide actins (heavy lines) and the biological selectivity isotherms (light lines). So ranked, the macrotetralide actins are from left to right trinactin, monactin, dinactin, nonactin. (Dinactin is out of place by such a ranking and the discrepancy could have been removed by ranking the data by the potassium-ammonium isotherm, for example. This would not alter any of the present conclusions.) The data at the right give the corresponding permeability ratios similarly ranked (the data points from left to right are for trinactin, dinactin, nonactin, monactin; and the heavy lines trace the average selectivities from the left hand side of the figure).

In sharp contrast to this is the cation selectivity pattern manifested by valinomycin illustrated in Fig. 19 where the precisely measured permeability ratios of Lev and Buzhinsky (1967, Table I, p. 103) at 23°C and pH 6·2–6·5 are plotted in the same manner as in Fig. 18. A remarkably close correspondence is immediately apparent between the permeability ratios characteristic of valinomycin (data points) for the alkali metal cations and those characteristic of cell membranes (curves).

The individual sets of data points correspond to the selectivities observed at different ionic strengths (from left to right 0·5 M, 0·2 M,

* The data in Figs. 18 and 19 have been located from left to right using the Rb^+ isotherm (i.e., the P_{Rb}/P_K ratio) since the selectivities of the macrotetralides for Na^+ are so different from the biological values that they cannot be scaled by the biological Na^+ isotherms. This procedure alters none of the conclusions to be drawn here.

0·1 M, 0·001 M and 0·01 M). Also included on the figure are the permeability ratios measured by Mueller and Rudin (1967) at 0·05 M ionic strength.* Why the permeability ratios for valinomycin should depend upon ionic strength is not clear. Nevertheless, the close agreement between these data (particularly for K, Rb, Cs and NH_4) and the biological specificity pattern is apparent. Such a dependence of the

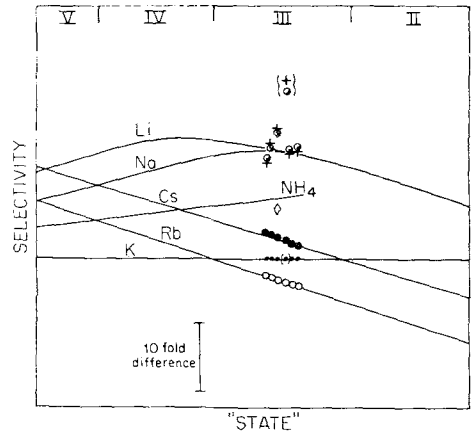

Figure 19. Comparison of the selectivity pattern for valinomycin with the cell membrane selectivity pattern. The data of Mueller and Rudin (1967) are indicated by parentheses. (See text for full details.)

"state" of the valinomycin molecule on ionic strength is not unprecedented. Similar changes in selectivity of glass electrodes, usually seen at constant ionic strength when pH is varied (Eisenman, 1962), are also observed at constant pH when salt concentration is varied.

Additional support for the similarities of ionic selectivity of valinomycin and of the cell membrane comes from close correspondence of the NH_4^+ selectivity data point for valinomycin plotted as a diamond in Fig. 19 (K_{NH_4}/K_K taken from the salt-extraction data of Table I is plotted, since membrane measurements for NH_4^+ are not presently available) and the NH_4^+ isotherm characteristic of the cell membrane. By contrast, the NH_4^+ selectivity for the macrotetralide actins of Fig. 18 are seen to be strikingly different from that of the cell membrane (and from valinomycin).

* The fact that Mueller and Rudin observed considerably lower Li and Na permeabilities (indicated by parentheses in Fig. 19) than did Lev and Buzhinsky, probably reflects the dependence of the apparent values of these permeabilities on trace components of other ions in the solution (see the discussion of Table II). The valinomycin permeability ratios at neutral pH give an overestimate of the effects of these ions on membrane potential due to the effects of H^+ among other cations. The important thing to note in Fig. 19 is that sodium and lithium permeabilities are considerably smaller than the potassium permeability. Indeed, they are probably considerably smaller than indicated both for the biological selectivity data and for the membrane selectivity data; and the apparent maximum and convergence of the Li and Na isotherms at the right of Figs. 16–18 probably reflects the effects of comparable levels of contaminating trace ions such as H^+ and K^+.

The above analysis of the quantitative differences in cation selectivity pattern between valinomycin and the macrotetralides indicate how sensitive the quantitative aspects of the cation-selectivity pattern are to the small differences in arrangements of the ligand groups in these two molecules. Indeed, we suggest that these patterns are useful as a "fingerprint" to distinguish between the sixfold carbonyl coordination of valinomycin and the four-fold coordinated carbonyl oxygens (and four-fold furane oxygens) present in the macrotetralide actins. For this reason we tentatively conclude that the cation detecting site in the resting cell membrane is not identical to that of the macrotetralide actins. It is tempting to speculate that it involves six carbonyl oxygens (possibly from the polypeptide backbone of a membrane protein) arrayed around the cation in a way essentially identical to the array characteristic of the interior of the cation-valinomycin complex.*

Irrespective of whether this speculation is correct or not, detailed comparisons of ionic specificity patterns are a powerful tool for inferring details of the likely ligand composition and configuration of the cation detecting sites in cell membranes and other biological molecules (e.g. cation-activated enzymes). The procedure is to compare the observed selectivity patterns in an unknown system with those characteristic of well defined model molecules of known ligand configuration (e.g. octahedral vs. tetrahedral) and type (e.g. carbonyl vs. ether) in the way illustrated here for cell membranes using valinomycin and the macrotetralides. A corollary is to infer the structure of the membrane's ligand groups from the selectivity of a membrane to particular "shapes" of cations. Hille (1971, 1972) has initiated such a characterization for the Na^+ and K^+ system of frog nerve.

Although the above considerations have been for passive permeation, the intracation selectivity pattern of Figs. 16 and 17 has been found to be the same as that seen in the active accumulation of ions in living cells, as well as in the cation activation of such enzymes as β-galactosidase and ATPase (Eisenman, 1965).

Energetics Underlying the Equilibrium Selectivity of Neutral Ion-Sequestering Molecules

Experiments described in the previous sections have examined the dependence for the observed membrane effects of valinomycin, the macrotetralides, and certain cyclic polyethers on the equilibrium

* It should be mentioned that, although the present selectivity considerations for the cell membrane are most easily deduced for a carrier mechanism of ion permeation, they are not at all inconsistent with the properties of a possible channel, whose selectivity could be due to either equilibrium or nonequilibrium factors. For example, if the process of loading and unloading of a channel is analogous to forming and dissociating a complex in water, the equilibrium selectivity factors, thought from the present analysis to underlie the ion interaction with molecules like valinomycin, could correlate with appropriate combinations of rate constants.

constants of certain simple reactions. In particular, identity (14), relating the ratios of membrane permeabilities and membrane conductances, salt extraction equilibrium constants, and aqueous complex formation constants has been verified experimentally:

$$\frac{P_j}{P_i} = \frac{G^0(\mathrm{J})}{G^0(\mathrm{I})} \simeq \frac{K_j}{K_i} \simeq \frac{K_{js}^+}{K_{is}^+}, \tag{14}$$

Since this result indicates that equilibrium considerations suffice to account for the principal effects of these molecules in bilayer membranes,* we will now examine the underlying equilibrium energetics in order to show how the energies contribute to the selectivity manifested in the effects of these molecules on bilayers. More detailed considerations of the energetic analysis of ionic selectivity will be found in papers by Simon and Morf (1972), by Eigen and his colleagues (Diebler *et al.*, 1969; Eigen and Winkler, 1971), and by Eisenman *et al.*, 1972, and Szabo *et al.*, 1972.

The formal relationships between the homogeneous reaction to form complexes in water and the heterogeneous reaction to solubilize cations in membranes (and salts in bulk phases).

From equilibrium considerations alone, the key to the selectivity of the present molecular carriers of cations lies in their ability to solubilize cations in media of low dielectric constant such as the interior of a phospholipid bilayer membrane. The cation solubilization can be expressed formally through equation (24) for the heterogeneous equilibrium by which a carrier molecule in the membrane, S^*_{memb}, reacts with a cation from the aqueous solution, I^+_{aq}, and solubilizes it in the membrane as the lipid soluble complex, IS^{+*}_{memb}:

$$I^+_{aq} + S^*_{memb} \underset{}{\overset{\bar{K}_i}{\rightleftharpoons}} IS^{+*}_{memb} \tag{24}$$

For clarity the subscripts "aq" and "memb" have been used to designate that the ions I^+ come from the aqueous phase whereas the

* It should also be noted that according to recent studies by Eigen's group (Diebler *et al.*, 1969) the ratio of the equilibrium constants for the formation of the complex in methanol have been shown for monactin to bear a direct relationship to the rate constant for loading the complex, $\vec{K}^+_{is}$, and the backward reaction of unloading the complex, $\overleftarrow{K}^+_{is}$, as defined in the reaction (written here for water):

$$I^+_{aq} + S^+_{aq} \underset{\overleftarrow{K}^+_{is}}{\overset{\vec{K}^+_{is}}{\rightleftharpoons}} IS^+_{aq}; \qquad K^+_{is} = \frac{\vec{K}^+_{is}}{\overleftarrow{K}^+_{is}} \tag{22}$$

where forward and backward rate constants have been indicated by arrows in the appropriate direction. The data of Diebler *et al.* in methanol suggest that the rate of formation of the complexes in water is diffusion controlled so that these rates are approximately the same for all cations. From this it is immediately possible to deduce that the ratio of formation constants must equal the ratio of the off constants for the kinetics of the reactions:

$$\frac{K^+_{js}}{K^+_{is}} = \frac{\overleftarrow{K}^+_{js}}{\overleftarrow{K}^+_{is}} \tag{23}$$

carrier molecules S and the complexes IS^+ are present in the membrane phase. (Although redundant, asterisks have been retained to designate species in the membrane for consistency with our previous publications.) The process by which this reaction enables ions to cross the membrane is indicated diagrammatically in Fig. 20. Equation (24) is an heterogeneous reaction, describing formally the process by which the IS^+ complex is formed within the membrane phase from a cation I^+ from the aqueous solution and a carrier molecule S from the membrane phase.*

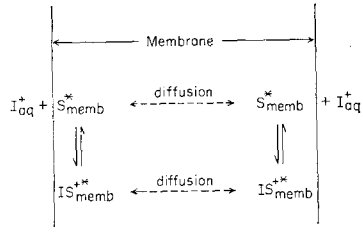

Figure 20. Diagram illustrating the process by which cations from the aqueous phase can react with carrier molecules from the membrane to form mobile complexes within the membrane.

This reaction is closely related to the reaction for extracting salt into an organic phase:

$$I^+_{aq} + X^-_{aq} + S^*_{memb} \underset{K_i}{\rightleftharpoons} IS^{+*}_{memb} + X^{-*}_{memb} \qquad (25)$$

differing from it only by the partition of the anion into the organic phase to preserve electroneutrality (see Ciani *et al.*, 1969 and Eisenman *et al.*, 1969 for further details).

The similarities between the heterogeneous reactions (24) and (25) are intuitively apparent. Less apparent, but equally real, is the similarity between these reactions and the homogeneous reaction (26) for the formation of the ion-carrier complex in water:

$$I^+_{aq} + S_{aq} \overset{K^+_{is}}{\rightleftharpoons} IS^+_{aq} \qquad (26)$$

This relationship is made more apparent by noting that reaction (24) can be viewed as the result of adding the subreaction (27) to, and subtracting subreaction (28) from, reaction (26).

$$IS^+_{aq} \overset{k_{is}}{\rightleftharpoons} IS^{+*}_{memb} \qquad (27)$$

$$S_{aq} \overset{k_s}{\rightleftharpoons} S^*_{memb} \qquad (28)$$

* Of course, this particular heterogeneous reaction cannot be distinguished in an equilibrium system from an alternative reaction path by which the IS^+ complex is formed in the aqueous phase and is then partitioned into the solvent. Stark and Benz (1971) have recently attempted to distinguish between these two possibilities, and a detailed theoretical analysis has been carried out by Ciani, Eisenman, Laprade and Szabo (1972) and is being tested experimentally in our laboratory by Raynald Laprade.

Reaction (27) represents the process of taking an IS^+ complex from an aqueous medium into the interior of the membrane; and its equilibrium constant, k_{is}, is the partition coefficient of the complex. Reaction (28) represents the process of taking a neutral molecule from an aqueous medium into the membrane, and its equilibrium constant, k_s, is the partition coefficient of the neutral carrier.*

Corresponding to these combinations of reactions, the equilibrium constant, $\bar{K}_i$, of the important heterogeneous reaction 24 is related to that, K_{is}^+, of the homogeneous equilibrium 26 through:

$$\bar{K}_i = K_{is}^+(k_{is}/k_s) \tag{29}$$

where K_{is}^+ is multiplied and divided by the equilibrium constants of reactions (27) and (28), respectively.

Taking the ratio of the equilibrium constants in equation 29 for two cations, J^+ and I^+, we get:

$$\frac{\bar{K}_j}{\bar{K}_i} = \frac{K_{js}^+}{K_{is}^+}\frac{k_{js}}{k_{is}}, \tag{30}$$

which, recalling equation (8) is seen to be identical to the ratio of K_j/K_i measured from salt extraction equilibria. This shows the basic identity:

$$\frac{\bar{K}_j}{\bar{K}_i} = \frac{K_j}{K_i}, \tag{31}$$

which constitutes the rationale for using measurements of bulk phase salt extraction equilibrium constants to deduce the properties of thin membranes and allows us to generalize equation (14) as:

$$\frac{\bar{K}_j}{\bar{K}_i} \simeq \frac{K_j}{K_i} \simeq \frac{K_{js}^+}{K_{is}^+} = \frac{P_j}{P_i} = \frac{G^0(\mathrm{J})}{G^0(\mathrm{I})} \tag{32}$$

Because of identity (32), we can consider the salt extraction equilibrium constant ratios, K_j/K_i, to give a measure either of the quantity $\bar{K}_j/\bar{K}_i$ or of K_{js}^+/K_{is}^+. Let us therefore consider the equilibrium factors underlying the selectivity of the homogeneous complex formation reaction (26), which is the simplest case with which to begin an analysis of the origin of the selectivity of the macrocyclic molecules at equilibrium.

Free Energy and Equilibrium Selectivity for the Formation of Ion-Carrier Complexes in Aqueous Solutions

The problem of understanding the equilibrium selectivity of any reaction is always one of assessing the elementary interactions underlying the Gibbs free energy change of the reaction (cf. Eisenman, 1961, 1962, 1965). Thus, the equilibrium constant, K_{js}^+, of reaction (26) is

* Of course, each of these equilibrium constants can be expressed as the ratio of rate constants for the forward and backward reactions, but considerations of kinetics exceed the scope of this paper.

related to the standard free energy change, ΔF^0, of the reaction through:

$$\Delta F^0 = -RT \ln K_{is}^{+}; \tag{33}$$

and the elementary process underlying the selectivity of this reaction can be assessed by decomposing the reaction into elementary processes following a classical Born-Haber cycle (cf. Eisenman, 1961).* This cycle is illustrated in Fig. 21. Reaction 26 has been indicated at the bottom in the heaviest lettering; and process I consists of taking the cation, I^+, and the carrier molecule, S, out of the aqueous solutions into

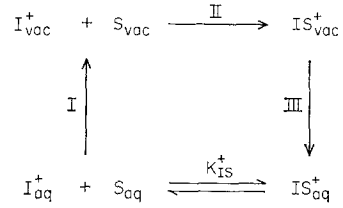

Figure 21. Born-Haber cycle decomposing the aqueous complex formation reaction into their conceptual subprocesses, as described in the text.

vacuum. Process II consists of allowing these species to combine in vacuum to form the IS^+ complex in vacuum. Process III consists of returning the IS^+ complex to the aqueous solution.

The free energy change for the overall reaction is given by the sum of these three subprocesses:

$$\Delta F_0 = -RT \ln K_{is}^{+} = \Delta F_{\mathrm{I}} + \Delta F_{\mathrm{II}} + \Delta F_{\mathrm{III}} \tag{34}$$

Let us now consider the separate contributions to these free energies.

The free energy of reaction I consists of the combination of the free energies of hydration of the cation, $\Delta F_{\mathrm{hyd}}(I^+)$, and of the neutral molecule, $\Delta F_{\mathrm{hyd}}(S)$;

$$-\Delta F_{\mathrm{I}} = \Delta F_{\mathrm{hyd}}(I^+) + \Delta F_{\mathrm{hyd}}(S). \tag{35}$$

$\Delta F_{\mathrm{hyd}}(I^+)$ can be assessed from the experimentally well known hydration energies of cations plus anions, provided an assumption is made as to the relative contribution between cation and anion (usually we are concerned only with the well-defined differences in the hydration energies for pairs of cations so that this assumption is generally not a problem). $\Delta F_{\mathrm{hyd}}(S)$ is an unknown quantity.

The free energy change of process II represents the free energy change in sequestering an ion inside the carrier molecule. This contains positive attractive terms between the cation and the ligand oxygens of the molecule as well as repulsive terms between ligand oxygens and

* It is important to note that since the system is at equilibrium, the free energy difference between the initial and final states are independent of the pathway taken between those two states. This fact justifies the use of the Born-Haber cycle as well as the use of alternative pathways further on in this section.

each other. These will be lumped together and called the "electrostatic" free energy, ΔF_{el}. In addition, there are strain energy differences between the conformation of uncomplexed carrier vs. the conformation of the complexed carrier as well as entropy changes, which are difficult to assess, all of which will be included in $\Delta F_{conform}$. So that:

$$\Delta F_{II} = \Delta F_{seq}(I^+) = \Delta F_{el}(I^+) + \Delta F_{conform}(I^+) \tag{36}$$

The free energy change of process III can also be considered to consist of two parts:

$$\Delta F_{III} = \Delta F_{Born}(IS^+) + \Delta F_{Cav}(IS^+) \tag{37}$$

where, $\Delta F_{Born}(IS^+)$ represents the electrostatic energy of the Born charging process for the IS^+ complex in aqueous media vs. vacuum (since the complex is quite large, the applicability of the Born charging process for a homogeneous dielectric should be a good approximation for this energy). $\Delta F_{Cav}(IS^+)$ represents the energy of forming a cavity in water around the IS^+ complex. If one wanted to evaluate the difference in free energy for the formation of an ion-carrier complex in the aqueous phase, therefore, one would need to know the values for the differences in free energies for each of the subcomponents of the equation

$$\begin{aligned} -RT\ln K_{is}^{+} = &-\Delta F_{hyd}(I^+) - \Delta F_{hyd}(S) + \Delta F_{el}(I^+) + \Delta F_{conform}(I^+) \\ &+ \Delta F_{Born}(IS^+) + \Delta F_{Cav}(IS^+) \end{aligned} \tag{38}$$

Although it could turn out that some of these energies are insignificant relative to others or that some of the terms cancel, not enough is known about the conformation of the molecule in these states to make the assumptions necessary to reduce this equation to any simpler form. By contrast, however, one can reduce the comparable equation for the selectivity ratio between two cations to a calculable form since, in this case, several of the terms will be the same, or sufficiently similar, that they will cancel. The following is the total equation for the difference in free energy of a carrier complexed with $[I^+]$ vs. $[J^+]$ before any terms are cancelled:

$$\begin{aligned} -RT\ln\frac{K_{js}^{+}}{K_{is}^{+}} = &\overbrace{-[\Delta F_{hyd}(J^+) - \Delta F_{hyd}(I^+)]}^{A} - \overbrace{[\Delta F_{hyd}(S) - \Delta F_{hyd}(S)]}^{B} \\ &+ \overbrace{[\Delta F_{el}(J^+) - \Delta F_{el}(I^+)]}^{C} + \overbrace{[\Delta F_{conform}(J^+) - \Delta F_{conform}(I^+)]}^{D} \\ &+ \overbrace{[\Delta F_{Born}(JS^+) - \Delta F_{Born}(IS^+)]}^{E} + \overbrace{[\Delta F_{Cav}(JS^+) - \Delta F_{Cav}(IS^+)]}^{F}. \end{aligned} \tag{39}$$

It is immediately apparent that term B equals zero and thus falls out of the equation. Furthermore, if one makes the reasonable assumption that the IS^+ and the JS^+ complexes are "isosteric" (Eisenman *et al.*, 1969), an assumption for which there is experimental evidence for several carrier-cation complexes (see the discussion of "isostericity"), then term D equals 0 because the conformations of IS^+ and JS^+ are the same, term E equals 0 because the radii of the IS^+ and JS^+ complexes are the same,* and term F equals 0 because the size of the cavities made by the IS^+ and JS^+ complexes are the same. For "isosteric" complexes, therefore, equation 39 reduces to

$$-RT\ln\frac{K_{js}^{+}}{K_{is}^{+}} = [\Delta F_{\text{hyd}}(I^+) - \Delta F_{\text{hyd}}(J^+)] - [\Delta F_{\text{el}}(I^+) - \Delta F_{\text{el}}(J^+)] \tag{41}$$

This important relation, in which the selectivity ratio reflects the differences in hydration energies of the cation species vs. the differences in their essentially electrostatic energies of sequestration within the antibiotic molecules in vacuum, underlies the analysis of the dipole model for antibiotic selectivity presented in the following section (cf. Eisenman, 1969; Eisenman *et al.*, 1972; Szabo *et al.*, 1972b).

Free Energy and Equilibrium Selectivity for Cation-binding by Membrane Carriers

If the reference state is taken as the hydrocarbon interior of a membrane rather than vacuum, a similar set of considerations can be applied for the key reaction 24 which describes the overall reaction by which the present carriers solubilize cations in a membrane.

To do this it will be helpful to refer to the physical states of the various cation complexing molecules and complexes in three different physical states schematized in Fig. 22. These states are: in water at the bottom; in the hydrocarbon region of the membrane in the middle; and in vacuum at the top. These states are interconnected by processes whose energies can be assessed by a Born-Haber cycle as in Fig. 21. Each process is designated by an arabic numeral and a verbal description. For example, the process "1. Hydration of I^+" represents the process of taking the cation I^+ from infinite dilution in vacuum to infinite dilution in water. The polar ligand oxygens have been indicated diagrammatic-

* The equation for the Born charging energy for a monovalent species is

$$\Delta F_{\text{Born}} = -\frac{332}{2r}\left(\frac{1}{D_{\text{vac}}} - \frac{1}{D_{\text{H}_2\text{O}}}\right) = -\frac{332}{2r}\left(\frac{79}{80}\right) \tag{40}$$

where r is the radius of the complex, D_{vac} is the dielectric constant of a vacuum, which is equal to 1, $D_{\text{H}_2\text{O}}$ is the dielectric constant of water, which is equal to 80, and the energy is in kcals per moles when r is in angstroms. Note that ΔF_{Born} will be the same for complexes with the same radii.

ally by dark ellipses, and the possibility of a conformational change in the molecule is illustrated in processes labelled "Change of conformation."*

It is possible to use the states diagrammed in Fig. 22 to analyze the process underlying the reaction (24) which is schematically indicated by the process:

$$S^*_{memb} \xrightarrow{k_s} S_{aq} + I_{aq} \xrightarrow{K^+_{is}} IS^+_{aq} \xrightarrow{k_{is}} IS^{+*}_{memb} \qquad (42)$$

The equilibrium constant $\bar{K}_i$ of this overall reaction (for processes 5, 6 and 7) can be decomposed into the sum of free energies for the four

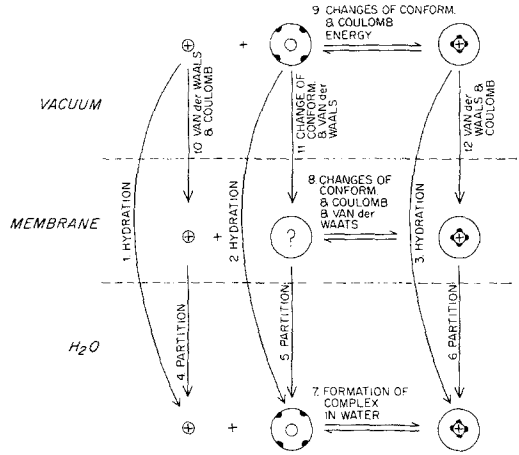

Figure 22. Diagram of the physical states of the various cation complexing molecules and their complexes.

processes (1, 11, 9 and 12 schematized in Fig. 22 such that $-RT \ln \bar{K}_i = -\Delta F_1 - \Delta F_{11} + \Delta F_9 + \Delta F_{12}$. The energies for these processes are as follows: ΔF_1 is the hydration energy of the cation. ΔF_{11} is the energy of taking the antibiotic molecule from vacuum into the membrane and contains an attractive (e.g. Van der Waals) interaction with the membrane interior (ΔF_{11a}) and a possible conformation change (ΔF_{11b}). ΔF_9 represents the ion sequestration reaction in vacuum, and has two parts: an attractive interaction (ΔF_{9a}), for which an electrostatic model will be given shortly, and a conformational energy change

* It seems reasonable to assume that the minimum energy configuration of the uncomplexed molecule will have the polar groups facing out in water. Similarly, it seems reasonable for the molecule to assume a similar configuration in vacuum since the polar ligand groups should exert repulsions on each other. It is difficult to predict, however, what configuration the uncomplexed molecule will have in the membrane since hydrophobic interaction between the hydrocarbons of the molecule and the hydrocarbons of the membrane would favor the same configuration as for the complexed molecule; whereas electrostatic repulsions between the carbonyl groups would favor the same configuration as for the uncomplexed molecule in vacuum. Hence the question mark on the figure. As none of these considerations is necessary when comparing one isosteric cation to another, since configurational effects then all cancel, we shall leave the configuration of the uncomplexed molecule in the membrane as undetermined.

(ΔF_{9b}). ΔF_{12} represents the differences of free energies of the complex in the membrane and in vacuum. This energy can be considered to consist of two parts: an electrostatic energy difference (ΔF_{12a}), and an attractive (e.g. Van der Waals) interaction energy between the complex and the membrane (ΔF_{12b}).

We can summarize these energies as follows:

$$-\Delta F_1 = -\Delta F_{\text{hyd}}(\text{I}^+)$$

$$-\Delta F_{11} = -\Delta F_{11a} - \Delta F_{11b} = -\Delta F_{\text{memb}}^{\text{Van der Waals}}(\text{S}) - \Delta F_{\text{memb}}^{\text{conformation}}(\text{S})$$

$$\Delta F_9 = \Delta F_{9a} + \Delta F_{9b} = \Delta F_{\text{vac}}^{\text{attractive}}(\text{IS}^+) + \Delta F_{\text{vac}}^{\text{conformation}}(\text{IS}^+)$$

$$\Delta F_{12} = \Delta F_{12a} + \Delta F_{12b} = \Delta F_{\text{memb}}^{\text{Born}}(\text{IS}^+) + \Delta F_{\text{memb}}^{\text{Van der Waals}}(\text{IS}^+).$$

Analogous with the previous calculation, there is not enough information known to reduce these equations to any simpler form; but if one looks instead at the relative selectivity between two cations, and assumes "isostericity", terms 11, 9b and 12 cancel for the two ions, and one is left with

$$-RT\ln\frac{\bar{K}_j}{\bar{K}_i} = [\Delta F_{\text{hyd}}(\text{I}^+) - \Delta F_{\text{hyd}}(\text{J}^+)] - [\Delta F_{\text{attractive}}^{\text{vac}}(\text{IS}^+) - \Delta F_{\text{attractive}}^{\text{vac}}(\text{JS}^+)]. \tag{43}$$

Equation (43) is seen to contain the same terms as equation (41).

The problem of cation selectivity of antibiotics in membranes thus reduces to a problem of assessing the competition between the interaction energies between the antibiotic and the ions in vacuum vs. the hydration energies of the ions. Since the differences of hydration energies are well known quantities, the problem reduces to one of estimating the sequestration energy differences expected between two cations. It is to this problem that we now turn.

Electrostatic Calculations of Binding Energies

We will now extend a previous model for the selectivity of monopolar ion exchange sites (Eisenman, 1961, 1962, 1965) to neutral dipolar sites which are more appropriate as models for the carbonyl (or ether) oxygens, which are the ion-binding ligands in the macrocyclic antibiotics. The considerations here in no way imply an attempt to calculate the binding energies for particular molecules; rather we try to examine the most obvious energy terms.

Monopolar Sites

Let us begin by considering a highly simplified model (Eisenman, 1961, 1962) in which the molecular anionic ion exchange sites of typical ion exchangers are approximated by a monopolar model, as indicated

diagrammatically in Fig. 23. Here we compare the selectivity expected for the competition for a given cation between such a site and a single water molecule. The energies of interaction of a monovalent cation I^+ of radius r^+ with a singly charged anionic site of radius r^-, referred to

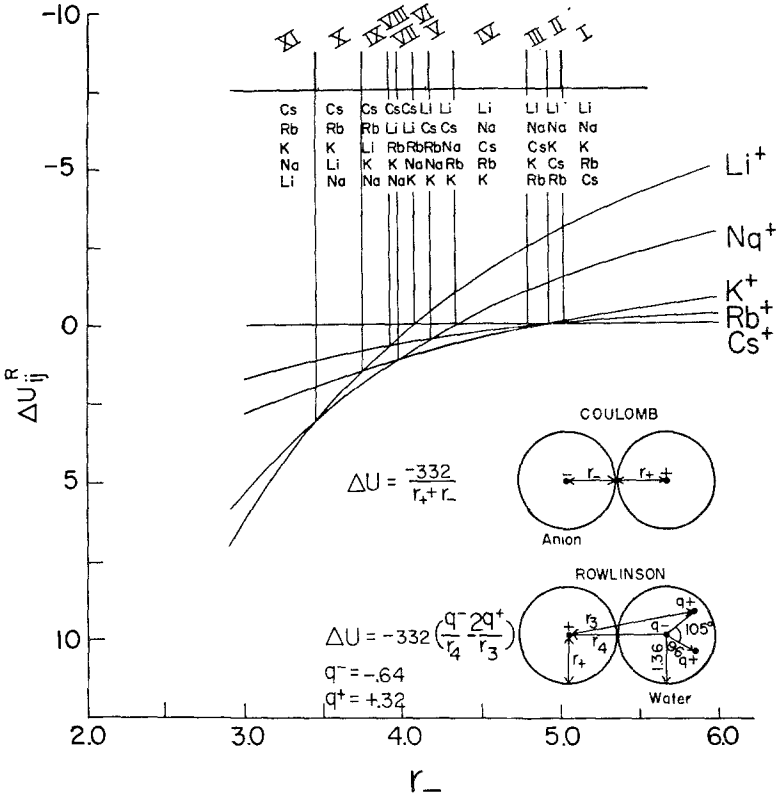

Figure 23. Selectivity pattern for the hypothetical cation exchange between a monopolar anion and a single multipolar water molecule. (Reproduced from Fig. 1 of Eisenman, 1961). The cation most strongly selected from water by the anionic "site' 'is the lowest on the chart. Above the graph are tabulated the cationic sequences (increasing specificity downwards), eleven rank order designations, as a function of decreasing site radius r_-. Units in kcal/mole and angstroms.

the ions at rest in a vacuum, are given approximately by the electrostatic attractive energy:

$$\Delta F_{\text{vac}}^{\text{attractive}} = \frac{-332}{r^+ + r^-} \tag{44}$$

While its energy of interaction with the indicated tripolar model of a water molecule is given by:

$$\Delta F^{\text{hyd}} = -332\left(\frac{q^-}{r_4} - \frac{2q^+}{r_3}\right), \tag{45}$$

representing the net attractions between the cation and the effective charge of the oxygen ($q^- = -0{\cdot}64$) at a distance r_4 from the center of the cation and the repulsions between the cation and the effective charge ($q^+ = +0{\cdot}32$) of the two protons at the greater distance r_3 from the center of the cation. (All energies are in kcal/mole for distances in angstroms, and charges are expressed as fractions of the electronic charge).

Calculating the values of these energies for the various naked (Goldschmitt) radii of the cations and inserting these in equation (41) (or 43),* one obtains the selectivity isotherms, referred to Cs^+, plotted on the ordinate in Fig. 23 (where energy in kcal/mole is labelled U_{ij}^r). This simple procedure leads to a pattern of selectivity in which, for the anion site of largest radius (i.e., lowest electrostatic field strength), the cations are preferred in the lyotropic sequence Cs > Rb > K > Na > Li while for an anionic site of sufficiently small radius the sequence of preference is reversed, being Li > Na > K > Rb > Cs. Between these extremes, the cations are seen to pass through eleven selectivity sequences, corresponding to the 11 Roman numerals designating the regions between the intercepts of the selectivity isotherms of Fig. 23.

This simple model is sufficient to account for the observed selectivities of many phenomena (as has been shown elsewhere in considerable detail (Eisenman, 1962, 1963, 1965; also see the excellent reviews by Reichenberg, 1966, and by Diamond and Wright, 1969). It can be made more realistic by replacing the interactions with the single water molecule by the differences of free energies of hydration of the cations in water, recalling that the interactions of cations with water are constant, being well known experimentally.†

Considering one limiting case, in which the sites of the exchanger are assumed to be widely separated and the water molecules are assumed to be excluded from their vicinity, the difference in free energies of interaction between cation and site ($\Delta F_{j+}^{\text{attract}} - \Delta F_{i+}^{\text{attract}}$) may be approximated by Coulomb's law (equation (44)). The selectivity expected in this case is plotted in Fig. 24.

In another limit, in which the sites are assumed to be very closely spaced (for example, with 6 sites coordinated around each cation and 6 cations around each site), the free energies are approximately given by

$$\Delta F_{\text{vac}}^{\text{attract}} = 1{\cdot}56\frac{-332}{r_+ + r_-} \tag{46}$$

where the factor 1·56 appears as a consequence of the Madelung con-

* Equations 41 and 43 are formally identical to the equation previously used for assessing the selectivity of monopolar ion exchangers.

† In these calculations, free energies of hydration were taken from Latimer's (1952) compilation as the most accurate source. Referred to Cs^+ these are: 53·8 ± 1·4 kcal/mole for Li^+, 28·9 ± 0·9 for Na^+, 12·7 ± 0·9 for K^+, and 6·7 ± 1·1 for Rb^+.

stant (1·75) for this coordination state and a factor of 8/9 due to the Born repulsion energy.* The expected selectivities in this case are plotted in Fig. 25.

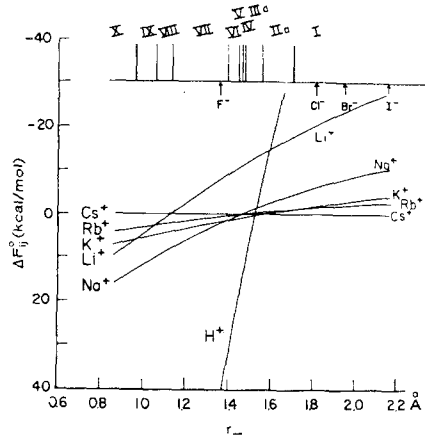

Figure 24. Selectivity isotherms for widely separated monopolar ion exchange sites. (Reproduced from Fig. 16 of Eisenman, 1962). Negative values of free energy change of reaction 30 of Eisenman, 1969 are plotted as a function of r_- for the case of widely separated sites. The Roman numerals above the figure indicate the sequences of ionic selectivity pertaining to the regions separated by the vertical lines drawn to the intersections of the various cation isotherms. The more strongly an ion is preferred by the exchanger the lower its position on the figure.

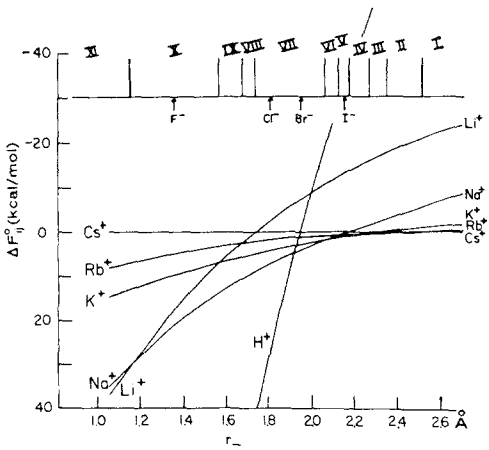

Figure 25. Selectivity isotherms for closely spaced monopolar sites. (Reproduced from Fig. 17 of Eisenman, 1962.) Plotted in the same manner as Fig. 24.

Inspection of Figs. 23–25 yields the following conclusions. First, the selectivity among cations depends in the same general way upon the

* Equation (46) is the classical Born-Lande equation for the internal energy of an alkali halide crystal lattice.

radius of the anion r_-, regardless of the differences in coordination of sites and waters. Second, a particular pattern is seen for the selectivity among group Ia cations in which only 11 sequences of cation effectiveness, indicated by the Roman numerals I to XI above the figures, are predicted out of a possible 120 permutations, with only the minor variations indicated by subscript "a". The underlying reason for this selectivity is the asymmetry between ion-site and ion-water interactions. Such an invariance of pattern is expected from the fact that the independent variable in these three figures is r_-, whereas the variable in the electrostatic term is $(r_+ + r_-)$. Since r_- is generally a quantity of the size of, or larger tham, r_+, any multiplication operation on the hydration energies or the electrostatic energies can always be approximately compensated for by a pure change in r_-. Indeed, if r_+ had been negligible compared to r_-, such changes in coordination number would have made no variations whatsoever in the pattern, since they could always be compensated for by merely shifting the magnitude of r_-. It is this basic asymmetry which underlies the ubiquitousness of the particular cation selectivity pattern in a wide variety of natural phenomena. It reflects the underlying fact that cation-site forces decrease more slowly with increasing distance than do cation-water forces (because water forces are essentially multipolar). Serious deviations from the above pattern are only expected when the ion interactions with the site fall off as a more rapid function of ion radius than their interactions with water. Such a situation occurs with a high atomic or molecular polarizability, as has been discussed in considerable detail elsewhere (Eisenman, 1961, 1962).

The applicability of this model has recently been critically assessed for ion exchangers by Reichenberg (1966), for zeolites by Sherry (1969), and for biological membranes by Diamond and Wright (1969).

Dipolar Sites

An understanding of the elementary factors underlying the specificity of neutral molecules which bind actions can be gained by extending the above considerations to a model illustrated in Fig. 26 for the carbonyl or ether oxygens which are the ligands in typical neutral carrier molecules.

For such a neutral dipolar site the electrostatic free energy is given by:

$$\Delta F_{\text{vac}}^{\text{attract}} = \left[\frac{-332}{r_+ + r_n} + \frac{332}{r_+ + r_p}\right](q.N), \tag{47}$$

where q is the fractional value of electronic charge, N is the coordination number of the ligands, r_+ is the (Goldschmitt) cationic radius, and r_n and r_p are the distances from the surface of the dipole of the negative and positive charges, respectively. (This calculation lumps all repul-

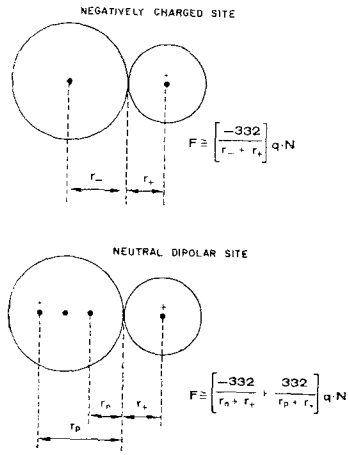

Figure 26. Models for a negatively charged ion exchange site and a neutral dipolar ligand. Described in text.

sions between ligands, as well as the Born repulsion with the cation, by diminution of effective charge.)

Calculating values for these energies and inserting in equations (41) and (43), using Latimer's (1952) experimental values for $\Delta F_{i+}^{hyd} - \Delta F_{j+}^{hyd}$, the selectivity isotherms of Fig. 27 were deduced.

Each subfigure in Fig. 27 presents a set of isotherms. The ordinate of each subfigure is the free energy change, as given at the lower left in

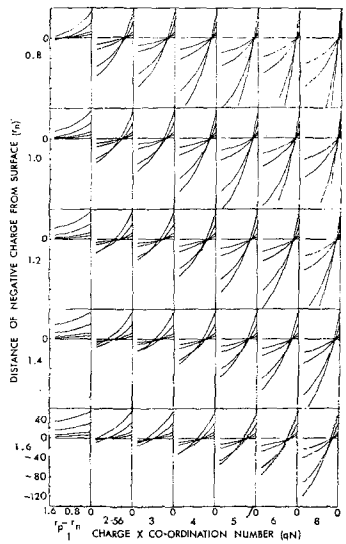

Figure 27. Selectivity isotherms for a neutral dipolar site as a function of various charge distributions and ligand coordination numbers. Described in text.

kcal/mole. The lower the position of the cation, the more it is preferred. The abscissa of each subfigure represents the separation (in Å) of the positive pole from the negative pole ($r_p - r_n$). This separation is zero at the right-hand side of each subfigure, in which case there is zero energy of interaction with the dipole; and the values of energies along the right-hand edge of each subfigure are therefore simply the differences of free energies of hydration, which are the same for all subfigures. The individual isotherms are not labelled but can be identified as follows: in all cases the horizontal line represents Cs^+, while the sequence of isotherms from bottom to top at the right-hand edge of each subfigure is Cs^+, Rb^+, K^+, Na^+, Li^+ (corresponding to the differences of free energies of hydration).

Each row of isotherms was calculated for a given distance of the negative pole from the surface (i.e., "0·8" means $r_n = 0{\cdot}8$ Å); while each column of isotherms corresponds to a particular product of charge times coordination number ($q.N$), as indicated at the bottom of the figures. (A value ($q.N$) equal to 3 could correspond to dipoles of unit charge in three-fold coordination or to dipoles of charge 0·5 in six-fold coordination.) These ranges of ($q.N$), r_n, and r_p should encompass all values of dipoles likely to be encountered for carbonyl or ether oxygens in nature (the family of isotherms for the value ($q.N$) of 2·56 represents a reasonable case of a tetrahedral coordination of ether oxygens having a net negative charge of −0·64 corresponding to the Rowlinson-type water molecule of Fig. 23). It has been assumed that the ligand oxygens of the sequestering molecules are free to coordinate around the naked cation with negligible steric restraints, at least from one cation to another.*

When the dipole separation is sufficiently large ($r_p - r_n \gg r_n$), the selectivities must approach those for the monopolar model, since in this situation the energetic contribution due to the positive pole becomes negligible. It is not surprising to see a pattern of selectivity sequences in Fig. 26 like those of the monopole model for this charge distribution. Of more interest is the fact that over a considerable range of dipolar charge distributions, the sequences of cation selectivity seen in Fig. 27 are essentially the same as those given by the monopolar model (cf. Figs. 23–25).

This similarity is in accord with the experimentally observed selectivities for the macrocyclic molecules. Thus, sequence IV ($K^+ > Rb^+ > Cs^+ > Na^+ > Li^+$) is observed for the macrotetralide actins (see Table III and figures 8 and 9) and sequence III ($Rb^+ > K^+ > Cs^+ > Na^+ > Li^+$) for valinomcyin (see Table II). Pressman (1968) has reported sequence IIa for the solvent extraction of compound X-537, sequence V for compound X-206 and nigericin, and sequence VII for dianemycin. Sequences III, IV, and VIII are apparent in Pedersen's (1968)

* For some molecules the key variable may be differences in coordination number.

published solvent extraction data for different cyclic polyethers; Lardy and his colleagues (1967) have found similar sequences for the effects of these compounds on biological membranes. Further data for macrocyclic molecules are summarized by Diamond and Wright (1969, pp. 587–588).

In considering the selectivity of an antibiotic such as nonactin or valinomycin (or for that matter, the selectivity of a biological site) it is useful to view N in Fig. 26 (i.e. the coordination number) as a variable which is a function of the radius of the complexed cation. As a specific example, it is probably unrealistic, because of steric considerations, to imagine that eight oxygens could be close-packed around a Li^+ ion whereas it is totally reasonable to expect that eight oxygens could be close-packed around a Cs^+ ion (cf. Pauling, 1960 for a discussion of closest packing arrangements). Therefore, a molecule such as nonactin might have the four carbonyl oxygens closely packed against Li^+ and the four tetrahydrofuran oxygens at a greater distance, whereas all eight oxygens might be closely packed against Cs^+. Similarly, valinomycin might have all six of its coordinating oxygens closely packed around Rb^+ and Cs^+ whereas only four of these oxygens may be able to pack closely around K^+, Na^+, and Li^+, the other two having to be at a greater distance (or, alternatively, the minimum energy configuration might even involve a cavity larger than the coordinated cation or even involve a coordination of partially hydrated cations). Additionally, the value of q in Fig. 26 (i.e. the charge on the ligand) is likely to be different for different ligand groups within a molecule (e.g. the value of q for the ester carbonyl oxygens in nonactin is likely to be different from the q value for the tetrahydrofuran oxygens in nonactin as well as differing from that for the amide carbonyl oxygens in valinomycin). Basically then, the product $q.N$ can be viewed as both a function of the complexing molecule and of the cation being complexed. A detailed calculation of such a case has not been done, but especially as the coordinations of the different cations in complexing molecules becomes known from crystallographic studies, such calculations might provide meaningful insights into the selectivity patterns for different antibiotics. Conversely, such calculations could also put constraints on the possible conformations of the ligand groups in biological cation binding sites.

It should therefore be apparent that the energies of interaction of cations with the dipolar ligand groups, in competitition with the hydration energies of the ions, can account for the salient features of the selectivity among the alkali metal cations characteristic of neutral sequestering molecules.

The realization of this basic competition between hydration energies and sequestration energies is important in interpreting selectivity data. For example, Prestegard and Chan (1970) noted a lack of selectivity in the binding manifested by nonactin in acetone solutions and therefore suggested "a rather similar dependence of the free energy of ion coordination on ion size for both nonactin and the solvent [acetone]".

It is likely that the ion size dependence of the relative energies of binding to nonactin carbonyls is sufficiently similar to that of the relative solvation energies by the acetone carbonyls that the apparent lack of selectivity is due to symmetrical interactions with the ligand groups vs. the solvent (see Szabo *et al.*, 1972). Indeed, their lack of selectivity suggests that carbonyl groups of acetone are excellent models for carbonyl groups of the macrotetralide actins.

The above realization also suffices to explain why it is that the ratios of stability constants for complex formation in a solvent such as methanol should bear a relatively simple relationship to the stability constants for the complex formation in water. That this is the case was previously discussed by Eisenman *et al.* (1970, see footnote 12, p. 340) where it was noted that this was understandable since the differences of solvation energies of cations in methanol are approximately the same as those in water and, from Fig. 22, it is apparent that the differences of Born charging energies for the complexes in methanol and water will also cancel. Therefore, the ratios of complex formation constants in methanol should indeed give a fairly accurate picture of the ratios of complex formation constants in water. This is a useful approximation since for most of the molecules of interest, the solubilities are not sufficiently high in water to measure these complex formation constants directly.

A discussion of selectivity of the present molecules would be incomplete without noting the importance of the spatial orientation assumed by the ligand groups. Although a detailed discussion of this lies beyond the scope of the present treatment, it is apparent from considerations of the unusually high ammonium ion selectivity for the macrotetralide actins (which have four carbonyl oxygens conveniently arrayed in tetrahedral coordination) as compared to the considerably lower ammonium selectivity of valinomycin (which has six carbonyl oxygens arrayed in octahedral symmetry), that the tetrahedral "shape" of the ammonium ion probably contributes an additional energy of interaction with the more suitably arrayed macrotetralide. Differences in details of the quantitative selectivity pattern among the essentially spherical alkali metal cations, and cations having definite "shape", such as ammonium, can provide empirical guide lines for attempting to decide the detailed array of the ligand groups (probably oxygens) of the binding sites in natural membranes.

Acknowledgement

It is a pleasure to acknowledge the perceptive and valuable comments and criticisms of our colleagues, Drs. Sally Krasne and Raynald Laprade.

References

Adelman, W. J. and Fok, Y. B., *J. Cell. Comp. Physiol.*, **64** (1964) 429.
Andreoli, T. E., Tieffenberg, M. and Tosteson, D. C., *J. Gen. Physiol.*, **50** (1967) 2527.

Baker, P. F., Hodgkin, A. L. and Shaw, T. I. *J. Physiol. (Lond.)* **164** (1962) 355.
Bean, R., in: *Membranes—A Series of Advances*, Vol. 2, G. Eisenman (ed.), Marcel Dekker, Inc., Publishers, New York.
Binstock, L. and Lecar, H. J., *Gen. Physiol.*, **53** (1969) 342.
Boyer, P. D., *Science*, **141** (1963) 1147.
Boyer, P. D., in: *Oxidases and Related Redox Systems*, Vol. 2, T. E. King, H. S. Manson and M. Morrison (eds.), Proc. Intern. Symp., Amherst, Mass., 1964, Wiley, New York, 1965.
Bright, D. and Truter, M. R., *Nature*, **225** (1970) 176.
Chance, B., in: *Energy Linked Functions of Mitochondria*, B. Chance (ed.), Academic Press, New York, 1963.
Chandler, W. K. and Meves, H., *J. Physiol. (Lond.)*, **173** (1964) 31; also *ibid.* **180** (1965) 788.
Ciani, S., Eisenman, G. and Szabo, G., *J. Membrane Biol.*, **1** (1969) 1.
Ciani, S., Eisenman, G., Laprade, R. and Szabo, G., in: *Membranes—A Series of Advances*, Vol. 2, Chap. 2, G. Eisenman (ed.), Marcel Dekker, Inc., Publishers, New York, 1972.
Cockrell, R. S., Harris, E. J. and Pressman, B. C., *Nature (Lond.)*, **215** (1967) 1487.
Colacicco, G., *J. Colloid and Interface Sci.*, **29** (1969) 345.
Diamond, J. M. and Wright, E. M., *Ann. Rev. Physiol.*, **31** (1969) 581.
Diebler, H., Eigen, M., Ilgenfritz, G., Maas, G. and Winkler, R., *Pure Appl. Chem.*, **20** (1969) 93.
Eigen, M. and Winkler, R., *Neurosci. Res. Program. Bull.*, **9** (1971) 330.
Eisenman, G., *Symposium on Membrane Transport and Metabolism*, A. Kleinzeller and A. Kotyk (eds.), p. 163. Academic Press, New York, 1961.
Eisenman, G., *Biophys. J.*, **2**, Part 2 (1962) 259.
Eisenman, G., *Bol. Inst. Estud. med. biol. (Mex.)*, **21** (1963) 155.
Eisenman, G., *Proc. of the XXIIIrd International Congress of Physiological Sciences (Tokyo)*, (1965) p. 489.
Eisenman, G., *Glass Electrodes for Hydrogen and Other Cations: Principles and Practice*, M. Dekker, New York, 1967.
Eisenman, G., *Federation Proc.*, **27** (1968) 6, 1249.
Eisenman, G., Ciani, S. M. and Szabo, G., *Federation Proc.*, **27** (1968) 6, 1289.
Eisenman, G., in: *Ion-Selective Electrodes*, R. A. Durst (ed.), National Bureau of Standards Special Publication 314, p. 1, 1969.
Eisenman, G., Ciani, S. M. and Szabo, G., *J. Membrane Biol.*, **1** (1969) 294.
Eisenman, G., McLaughlin, S. G. A. and Szabo, G., IUPAC Presymposium on "Physical Chemical Basis of Ion Transport Through Biological Membranes", Riga, U.S.S.R. (1970).
Eisenman, G., Szabo, G., Ciani, S., McLaughlin, S. and Krasne, S., *Progress in Surface and Membrane Science*, J. F. Danielli (ed.), Academic Press, 1972, in press.
Finkelstein, A., *Biochim. Biophys. Acta*, **205** (1970) 1.
Finkelstein, A. and Cass, A., *J. Gen. Physiol.*, **52** (1968) 145s.
Finkelstein, A. and Holz, R., in: *Membranes—A Series of Advances*, Vol. 2, G. Eisenman (ed.), Marcel Dekker, Inc., Publishers, New York, 1972.
Frensdorff, H. K., *J. Am. Chem. Soc.*, **93** (1971) 600.
Gilbert, D., (1970) See Stillman *et al.* (1969).
Goldman, D. E., *J. Gen. Physiol.*, **27** (1943) 37.
Goodall, M. C., *Biochim. Biophys. Acta*, **219** (1970) 28.
Green, D. E. and Perdue, J. F., *Ann. N.Y. Acad.. Sci.*, **137** (1966) 667.
Hille, B., *J. Gen. Physiol.*, **58** (1971) 599.
Hille, B., *J. Gen. Physiol.* **59** (1972) in press.
Hladky, S. B. and Haydon, D. A., *Nature*, **225** (1970) 451.
Hodgkin, A. L., *J. Physiol.*, **106** (1947) 319.
Hodgkin, A. L. and Katz, B., *J. Physiol.*, **116** (1949) 473.
Izatt, R. M., Nelson, D. P., Rytting, J. H., Haymore, B. L. and Christensen, J. J., *J. Am. Chem. Soc.* **93** (1971) 1619.
Jardetsky, O., *Nature*, **211** (1966) 969.
Kepes, A., *The Cellular Functions of Membrane Transport*, J. H. Hoffman (ed.), Prentice-Hall, New Jersey, 1964, p. 155.
Kilbourn, B. T., Dunitz, J. D., Pioda, L. A. R. and Simon, W., *J. Mol. Biol.*, **30** (1967) 559.
Krasne, S., Eisenman, G. and Szabo, G., *Science*, **174** (1971) 412.
Laprade, R., Szabo, G., Ciani, S. M. and Eisenman, G., *Abstracts, Biophys. Soc. Meeting*, 1972.
Lardy, H. A., Graven, S. N. and Estrada-O, S., *Fed. Proc.*, **26** (1967) 1355.
Läuger, P. and Stark, G., *Biochim. Biophys. Acta*, **211** (1970) 458.
LeBlanc, O. H., *J. Memb. Biol.*, **4** (1971) 227.
Lehninger, A. L., The Mitochondrion, Benjamin, New York, 1965.
Lesslauer, W., Richter, J. and Läuger, P., *Nature*, **213** (1967) 1224.
Lev, A. A., and Buzhinsky, E. P. *Tsitologiya*, **9** (1967) 102.
Liberman, E. A. and Topaly, V. P., *Biochim. Biophys. Acta*, **163** (1968) 125.
Liberman, E. A., Pronevich, L. A. and Topaly, V. P., *Biofizika*, **15** (1970) 612.

Ling, G. N., *A physical theory of the living state*, Blaisdell Publ. Co., Waltham, Mass., 1962.
Lipmann, F., in: *Currents in Biochemical Research*, D. E. Green (ed.), Interscience, New York, 1946, p. 137.
Markin, V. S., Krishtalik, L. I., Liberman, E. A. and Topaly, V. P., *Biofizika*, **14** (1969) 256.
Markin, V. S., Pastushenko, V. F., Krishtalik, L. I., Liberman, E. A. and Topaly, V. P., *Biofizika*, **14** (1969) 462.
McLaughlin, S. G. A., Szabo, G., Eisenman, G. and Ciani, S. M., *Proc. Natn. Acad. Sci.*, **67** (1970) 1268.
McLaughlin, S. G. A., Szabo, G., Ciani, S. and Eisenman, G., *J. Memb. Biol.* (1972). In Press.
Mitchell, P., *Nature*, **191** (1961) 144.
Mitchell, P., in: *Membranes and Ion Transport*, Vol. 1, E. E. Bittar, (ed.), Wiley, New York, 1971, p. 192.
Mueller, P. and Rudin, D. O., *Biochem. Biophys. Res. Commun.*, **26** (1967) 398.
Mueller, P. and Rudin, D. O., in: *Current Topics in Bioenergetics*, Vol. 3, Academic Press, New York, 1969, p. 157.
Neumcke, B., *Biophysik*, **6** (1970) 231.
Neumcke, B. and Läuger, P., *J. Memb. Biol.*, **3** (1970) 54.
Patlak, C. S., *Bull. Math. Biophys.*, **19** (1957) 209.
Pauling, L., *The Nature of the Chemical Bond*, Cornell Univ. Press, New York, 1960.
Pedersen, C. J., *J. Am. Chem. Soc.*, **89** (1967) 7017.
Pedersen, C. J., *Fed. Proc.*, **27** (1968) 1305.
Pedersen, C. J., *J. Am. Chem. Soc.* **92** (1970) 386.
Pressman, B. C., Harris, E. J., Jagger, W. S. and Johnson, J. H., *Proc. Natn. Acad. Sci.* **58** (1967) 1949.
Pressman, B. C., *Fed. Proc.* **27** (1968) 1283.
Prestegard, J. and Chan, S. I., *J. Amer. Chem. Soc.*, **92** (1970) 4440.
Reichenberg, D., in: *Ion Exchange*, Vol. 1, J. Marinsky (ed.), Dekker, New York, 1966, p. 277.
Shemyakin, M. M., Ovchinnikov, Y. A., Ivanov, V. I., Antonov, V. K., Vinogradova, E. I., Shkrob, A. M., Malenkov, G. G., Evstratov, A. V., Laine, I. A., Melnik, E. I. and Ryabova, I. D., *J. Memb. Biol.*, **1** (1969) 402.
Sherry, H. S., in: *Ion Exchange*, Vol. 2, J. Marinsky (ed.), Dekker, New York, 1969, p. 89.
Simon, W. and Morf, W., in: *Membranes—A Series of Advances*, Vol. 2, G. Eisenman (ed.), Marcel Dekker, Inc., Publishers, New York, 1972.
Skou, J. C., *Progress in Biophysics*, **14** (1964) 131.
Slater, E. C., *Nature*, **172** (1953) 975.
Stark, G. and Benz, R., *J. Membrane Biol.*, **5** (1971) 133.
Stillman, I., Gilbert, D. and Robbins, M., *Biophysical Society Abstracts*, A-250 (1969).
Szabo, G., Eisenman, G. and Ciani, S., *J. Memb. Biol.*, **3** (1969) 346.
Szabo, G., Eisenman, G. and Ciani, S. M., in: *Physical Principles of Biological Membranes*, F. Snell, J. Wolken, G. J. Iverson and J. Lam (eds.), Gordon and Breach Science Publishers, New York, 1970, (1970) pp. 79–133.
Szabo, G., Eisenman, G., Krasne, S., Ciani, S. and Laprade, R., in: *Membranes—A Series of Advances*, Vol. 2, Chap. 3, G. Eisenman, (ed.), Marcel Dekker, Inc., Publishers, New York, 1972.
Szabo, G., Eisenman, G., McLaughlin, S. G. A. and Krasne, S., *Ann. N.Y. Acad. Sci.*, **195** (1962a) 273.
Tosteson, D. C., *Fed. Proc.*, **27** (1968) 1269.
Urry, D. W., *Proc. Natn. Acad. Sci.*, **68** (1971) 672.
Whittam, R., *The Neurosciences*, G. C. Quarton, T. Melnechuk and F. O. Schmitt (eds.), 1967, p. 313.
Wipf, H. K., Pache, W., Jordan, P., Zähner, H., Keller-Schierlein, W. and Simon, W. *Biochem. Biophys. Res. Commun.*, **34** (1969) 387.